European Journal of Cell Biology 105 (2026) 151546

Contents lists available at ScienceDirect

European Journal of Cell Biology

journal homepage: www.elsevier.com/locate/ejcb

The plaque protein myozap defines unique junction strands in smooth muscle cell bundles☆

Werner W. Franke [a], Steffen Rickelt [a], Yvette Dörflinger [a], Caecilia Kuhn [a], Stefanie Winter-Simanowski [a], Ralf Zimbelmann [a], Adam Breitscheidel [b], Roland Moll [c,*], Rudolf E. Leube [b,*]

[a] German Cancer Research Center, Helmholtz Group for Cell Biology, Im Neuenheimer Feld 280, Heidelberg 69120, Germany
[b] RWTH Aachen University, Institute of Molecular and Cellular Anatomy, Wendlingweg 2, Aachen 52074, Germany
[c] Philipps-Universität Marburg, Fachbereich Medizin, Institute of Pathology, Baldingerstrasse, Marburg 35033, Germany

ARTICLE INFO

Keywords:
Myozap
Integrin
Smooth muscle
Cell-cell contact
Focal adhesion
Junction plaque
Caveola

ABSTRACT

In bundles of smooth muscle cells associated with mammalian organs of the urogenital and alimentary tract we have discovered and partly characterized a novel kind of mirror image-symmetrically organized cell-cell junctions which are not based on direct transcellular contacts of transmembrane proteins or surface glycoproteins but represent extensive plasma membrane regions coated with cytoplasmic plaque ridges. The parallel, regularly spaced, rather thick (25–40 nm) and mostly very long (often for the entire length of the cell) myofilament-anchoring plaques of these junctions contain not only the focal adhesion-associated proteins vinculin, plectin and talin but also abundant amounts of protein myozap recently discovered as a major component of the plaques of adherens junctions in epithelia and endothelia as well as of the composite junctions connecting cardiomyocytes. α5- and β1-integrins are identified as the most prominent transmembrane molecules of these special smooth muscle junctions. In contrast, the tetraspanin CD151 co-distributes only in part with the myozap-positive junctions. These junctions are furthermore negative for proteins of adhering junctions. The myozap-containing junctional strands alternate with caveolin/dystrophin-positive regions. Characteristically, these novel cell-cell junctions are separated by extracellular matrix including the basal laminae of the adjacent cells which frequently fuse to a single electron-dense lamella forming the symmetry plane. We propose that the myozap-containing junctional strands may have important mechanical functions enabling and coordinating the contraction of closely-packed smooth muscle cell bundles throughout the body.

1. Introduction

The four categories of bilaterally symmetrical cell-cell junctions are based on type-characteristic transmembrane molecules of the one cell binding directly and homotypically the same or a similar region of the adjacent cell: cadherin glycoproteins in the field of adherens junctions (AJs) and desmosomes, connexins in gap junctions as well as claudins in tight junctions (Farquhar and Palade, 1963); for review see (Franke, 2009; Goodenough and Paul, 2009; Schulzke et al., 2012). We now present evidence for the existence of junctions of another category that connect cells of bundled smooth muscle tissues and are arranged in long parallel strands. These junctions are based on transmembrane proteins of the integrin family, intersecting basal laminae in the symmetry plane and extended cytoplasmic plaques of a unique composition with protein myozap as a major and characteristic component. This protein, originally detected in the plaques of the composite junctions (*areae compositae*) connecting the cardiomyocytes in the intercalated disks of the mammalian heart (Frank et al., 2014; Seeger et al., 2010), was subsequently also identified as a general component of certain cadherin-based junctions of the AJ category, specifically in AJs of endothelial cells of the vascular system (Pieperhoff et al., 2012) and in the apical *zonulae adhaerentes* of epithelial cells and related AJ structures of tumors derived

☆ The data were collected by Werner Franke with the help of Steffen Rickelt, Yvette Dörflinger, Caecilia Kuhn, Stefanie Winter-Simanowski and Ralf Zimbelmann at the German Cancer Research Center. They were assembled by Roland Moll, Adam Breitscheidel and Rudolf E. Leube after Werner Franke passed away on November 14th, 2022.

* Corresponding authors.
E-mail addresses: mollr@staff.uni-marburg.de (R. Moll), rleube@ukaachen.de (R.E. Leube).

https://doi.org/10.1016/j.ejcb.2026.151546
Received 29 April 2026; Received in revised form 2 June 2026; Accepted 4 June 2026
Available online 6 June 2026
0171-9335/© 2026 The Authors. Published by Elsevier GmbH. This is an open access article under the CC BY license (http://creativecommons.org/licenses/by/4.0/).

therefrom (Rickelt et al., 2011). After we had succeeded in generating very sensitive and specific antibodies against protein myozap we had to recognize that this protein does not only occur in certain cell-cell junctions of the AJ type but also in the submembranous plaques of focal adhesion-type structures of a major type of mammalian smooth muscle cells. We show that junctions of this category can occupy large portions of the plasma membrane of the cells connected, up to half of the cell surface, and are characterized by a cytoplasmic plaque rich in protein myozap. To date, symmetric focal adhesion-like junctions have not been detected either in native tissues or cultured cells.

2. Materials and methods

2.1. Tissues

Human tissue samples were obtained in connection with diagnostics in pathology, in compliance with the regulations of the Ethics Committee of the University of Heidelberg (Germany), and cryopreserved as described (Langbein et al., 2003; Pieperhoff et al., 2012; Rickelt et al., 2011; Straub et al., 2011). Bovine, porcine and murine (rat and mouse) tissue samples were obtained from a regional slaughterhouse (Mannheim, Germany) or the laboratory animal facilities of the German Cancer Research Center (Heidelberg, Germany). The tissue samples were either cryopreserved or glutaraldehyde-fixed (for details see (Franke et al., 2006)).

Antibodies used for immunofluorescence and immunoelectron microscopy and for immunoblot analyses of gel-electrophoretically separated polypeptides are listed in Table 1.

Table 1
List of primary antibodies*.

Antigen	Clonality, Species (Designation)	Source (Ordering Number/ Reference)
N-cadherin (cadherin−2, CDH2)	mcl, m (clone 32)	BD Transduction Laboratories (610921)
Cadherin−11 (OB-Cadherin, CDH11)	mcl, m (clone 5B2H5)	Thermo Fisher Scientific (32–1700)
α-catenin (CTNNA1, αE-catenin)	mcl, m (alpha-CAT−7A4)	Thermo Fisher Scientific (13–9700)
β-catenin	mcl, m (clone 14)	BD Transduction Laboratories (610154)
Caveolin−1	mcl, rb (clone D46G3)	Cell Signaling (3267)
Collagen IV	pcl, rb	Progen Biotechnik (10760)
Dystrophin	pcl, rb	Abcam (ab15277)
a5-Integrin (CD49e)	mcl, m (clone IIA1)	BD Biosciences (555615)
ß1-Integrin (CD29)	mcl, rat (clone 9EG7)	BD Pharmingen (550531)
Myozap	mcl, m (clone 517.67)	Progen Biotechnik (651169)
	pcl, gp	Authors' laboratory (Rickelt et al., 2011; Seeger et al., 2010)
Plectin	pcl, gp	Progen Biotechnik (GP21)
p0071	pcl, gp	Progen Biotechnik (GP71)
Smoothelin	mcl, m (clone R4A)	Sigma-Aldrich (MAB3242)
Talin	mcl, m (clone TA205)	Sigma-Aldrich (SAB4200041)
Tetraspanin CD151	mcl, m (clone 11G5a)	Origene (SM1209P)
Vinculin	mcl, m (clone VIN−11–5)	Sigma-Aldrich (V4505)
ZO−1	mcl, m (clone ZO1–1A12)	Thermo Fisher Scientific (33–9100)

Abbreviations: mcl, monoclonal antibodies; pcl, polyclonal antibodies; m, mouse; rb, rabbit; gp, guinea pig.

* The list contains only the antibodies that have been used to prepare the figures displayed in the manuscript. Antibodies that showed a negative reaction in the myozap-positive smooth muscle cell bundles (i.e., antibodies directed against l/s-Afadin, E-Cadherin, P-Cadherin, Desmoplakin, Desmogleins 1–3, Desmocollins 1–3, α6-Integrin, Fibronectin, HD233, PERP, Plakophilins 1–3, Plakoglobin, Protein p120, ZO−2) are not listed but are referenced in (Domke and Franke, 2019).

2.2. Microscopy and immunolocalizations

Single and double-label confocal immunofluorescence microscopy was performed as suggested by the manufacturers of the antibodies and as described (Franke and Rickelt, 2011; Rickelt et al., 2011, 2010; Straub et al., 2011). Methods used for conventional and immunoelectron microscopy (immunogold-silver enhancement procedure) have also been described repeatedly (Pieperhoff et al., 2012; Rickelt et al., 2011, 2009).

2.3. Biochemistry

Tissue samples were processed and subjected to SDS-PAGE or two dimensional (2D)-PAGE, followed by transfer to PVDF membranes and immunoblot reactions as described (Borrmann et al., 2006; Franke and Rickelt, 2011; Pieperhoff et al., 2012; Rickelt et al., 2011, 2010; Straub et al., 2011).

2.4. 3D model development

The 3D model was designed with the help of the open source software Blender 5.0.

3. Results

3.1. Immunofluorescence microscopy detects the plaque protein myozap at cell borders of smooth muscle cell bundles of the urogenital and gastrointestinal tract

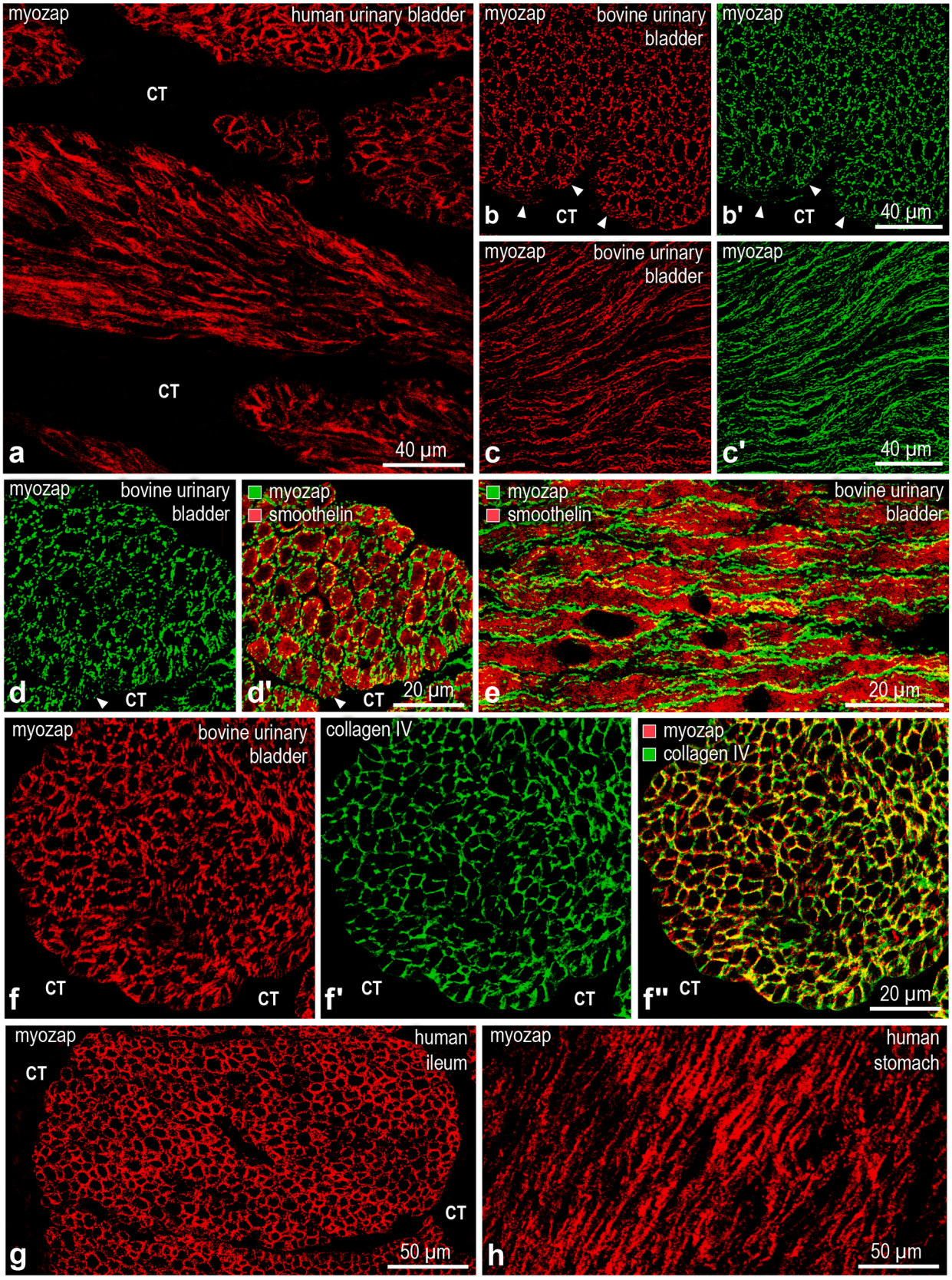
Using antibodies against myozap prominent immunofluorescence signals were detected in smooth muscle cells of the urinary bladder. Fig. 1a shows the anti-myozap fluorescence in cross and longitudinal sections of cells within smooth muscle cell bundles located in the outer portion of the human bladder wall. It presents distinct puncta at cell borders in cross sections and linear strands in longitudinal sections. The strands had often a dotted appearance indicative of local myozap accumulations. The same distribution patterns were observed in bovine urinary bladder (Fig. 1b-c′). Identical immunofluorescence was detectable using either monoclonal or polyclonal anti-myozap antibodies (compare Fig. 1b, c with Fig. 1b', c′; see also Fig. S1).

The double-label immunofluorescence microscopy of myozap and smoothelin in Fig. 1d-e demonstrates the muscle character of the cells. The abundant smoothelin staining is restricted to the cytoplasm and does not co-localize with the peripheral anti-myozap signal. On the other hand, the myozap signal codistributed in part with the basement membrane component collagen IV (Fig. 1f-f"). The latter, however, was evenly distributed completely surrounding individual smooth muscle cells (Fig. S2). Next to the prominent myozap staining of cell-cell contact regions, similar myozap-positive cell surface structures were also found in cell regions that were apparently not in direct contact with another cell (e. g., at the bundle periphery bordering connective tissue in Fig. 1b, b′, d and Fig. S1).

Structurally and compositionally very similar bundles of tightly-packed smooth muscle cells exhibiting prominent myozap immunostaining were also seen in the outer parts of various portions of the urogenital tract, from the ureter downward, in all mammalian species examined (not shown), as well as in various parts of the alimentary tract such as the esophagus, the stomach, all the intestinal intercepts and in the gall bladder wall and also in the tracheal walls of all species examined (not shown). For examples we show in Fig. 1g a near cross-section of a smooth muscle cell bundle of human ileum and in Fig. 1h a grazing section of the human stomach wall.

3.2. Immunoblotting detects multiple, cell type-specific isoelectric variants of myozap in mammalian muscle tissue samples

In biochemical experiments protein myozap could be detected in



(caption on next page)

Fig. 1. Myozap is localized in longitudinal junctional strands of smooth muscle cells in the urinary bladder, ileum and stomach. (a) Immunofluorescence microscopy of myozap in the muscle wall of human urinary bladder using monoclonal anti-myozap antibody. The fluorescence signals are localized at cell borders within bundles of smooth muscle cells whereas the surrounding connective tissue (CT) is devoid of fluorescence. Myozap immunoreactivity is concentrated in distinct puncta in cross sections (upper and lower parts) and in strands in longitudinal sections (middle). (b-c′) Double-label imunofluorescence microscopy of cryostat cross and longitudinal sections (b, b' and c, c', respectively) through snap-frozen smooth muscle tissue of bovine urinary bladder muscularis coat using a murine monoclonal antibody to protein myozap (b, c; red) and polyclonal guinea pig myozap antibodies (b', c′; green) that are directed to different myozap epitopes. Note the colocalization of both immunoreactivities. Note presence of myozap-positive puncta also at the interface to the extracellular matrix (arrowheads; see also Fig. S1). (d, e) Double-label immunofluorescence microscopy of a cross (d, d′) and a longitudinal (e) section through smooth muscle cell bundles of bovine urinary bladder coat tissue using murine monoclonal antibodies to smoothelin (red) and polyclonal guinea pig antibodies to protein myozap (green). Note that myozap is specific for - and thus restricted to - the cell border regions whereas smoothelin is present in the entire actomyosin-rich cytoplasm. Arrowhead, myozap-positive structure at border to surrounding connective tissue (CT). (f-f") Double-label immunofluorescence micrographs showing the colocalization of protein myozap (monoclonal murine antibodies; red) and the basement membrane-specific protein collagen IV (rabbit polyclonal antibodies; green) in a muscle cell bundle of bovine urinary bladder. Note the frequent "merger-like" interaction, resulting from the very close association of myozap and the extracellular basal lamina protein collagen IV ((f"); further details in Fig. S2). CT, connective tissue. (g, h) Exemplary fluorescence images showing the abundance and orientation of protein myozap-containing cell-cell border regions in smooth muscle cell fiber bundles stained by imunofluorescence microscopy using murine monoclonal antibodies to protein myozap in a cross section through an ileum wall muscle bundle (g) and a near longitudinal section through a stomach wall smooth muscle bundle (h). CT, connective tissue.

dissected tissue elements as well as in cytoskeletal enrichment preparations, prepared from human tissues or from tissues of other species. Myozap is a prominent component in human ureter, bladder, urethra, ductus deferens and the gall bladder but is absent in kidney tissue (Fig. 2a). Moreover, practically identical results were obtained when these tissues were compared in different vertebrate species including human, bovine, porcine and murine samples (Fig. 2b).

However, when the proteins from different tissues of the same species were compared by two-dimensional gel electrophoresis clear differences in the tissue-specific isoelectric variant patterns were apparent. A particularly impressive example was the difference between protein myozap from cardiac and urinary bladder tissue (Fig. 2c-e). While myocardial (intercalated disc) myozap revealed two major isoelectric variants (Fig. 2d), bladder myozap showed three additional more acidic variants resulting in altogether five variants (Fig. 2c; the co-electrophoresed mixture is shown in Fig. 2e).

3.3. *Electron microscopy reveals that myozap is localized in plaques of junctional strands in smooth muscle cells*

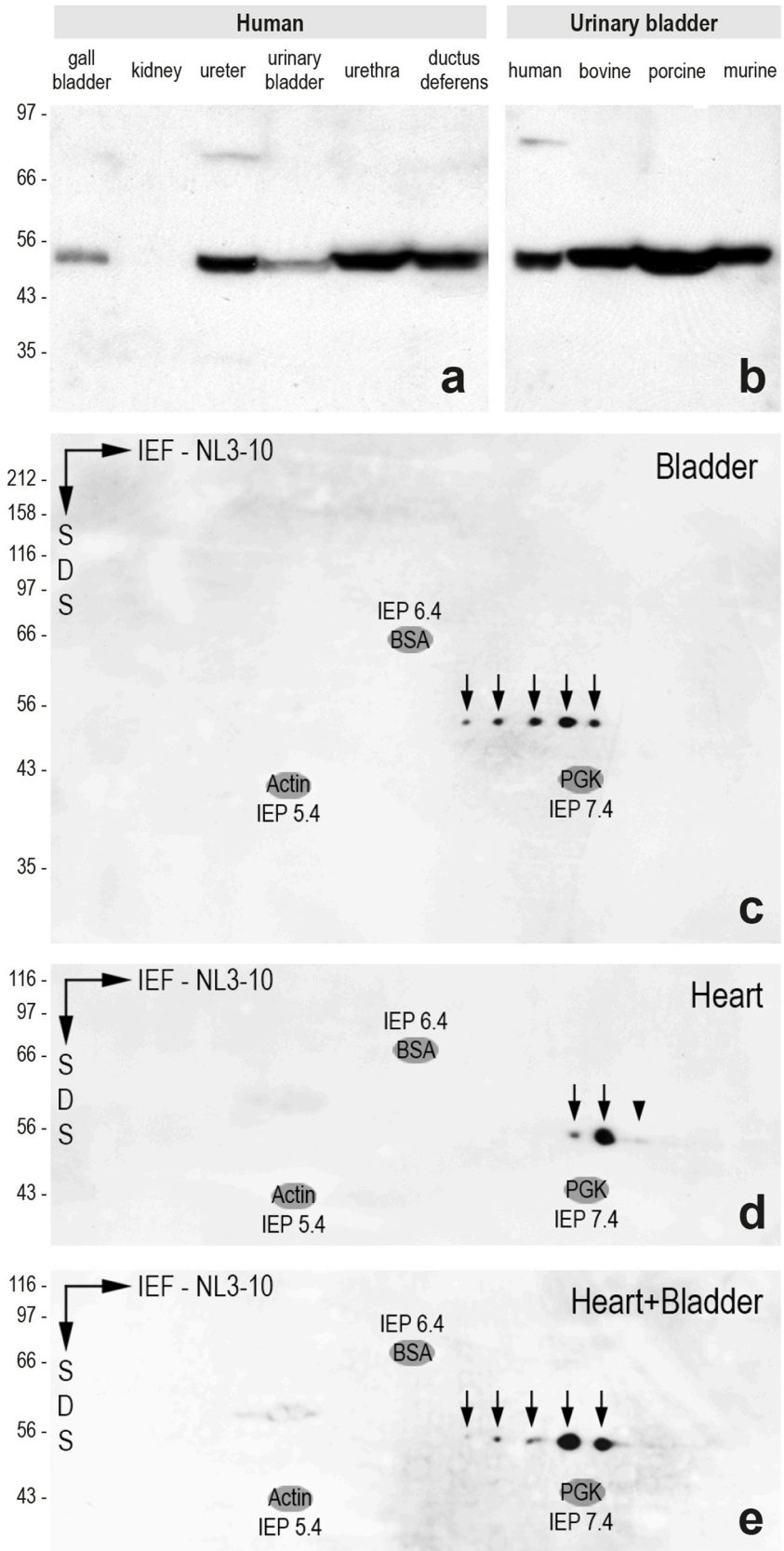
Immunoelectron microscopy was performed next to localize myozap in smooth muscle cells of bovine urinary bladder. Low magnification images in cross-sections revealed the characteristic organization of the mononuclear, mostly somewhat elongate rippled smooth muscle cells (Fig. 3a, b). The cytoplasm of these cells was densely packed with "thin" (actin-based) and " thick" (myosin-based) myofilaments which were often associated with cytoplasmic "dense bodies" typical for smooth muscle cells. Prominent dense plasma membrane plaques were detected in all smooth muscle cells studied, facing corresponding plaques in adjacent cells or facing the extracellular matrix (ECM), thus coating a considerable percentage of the inner aspect of the plasma membrane. In between plaque-coated membrane regions, some cortical regions showed accumulations of vesicles. The interspaces between the smooth muscle cells were often rather narrow but could be wider in other regions and physiological states and were filled to various degrees with ECM structures, including basal laminae and collagen fibrils.

Higher magnifications revealed that all plasma membrane-associated plaques were positive for myozap and that the regions in between were completely negative (Fig. 3c-g). Fig. 3c-f shows details of the electron microscopic appearance of the cell-cell connections in a state of close cell-cell adhesion. Here the plaque-coated membrane structures were either associated into complete, mirror-image symmetrical cell-cell contact elements or were only partly matched in "incomplete" associations. Frequently, in such contact regions single or double central middle lamellae were recognized resembling the basal laminae that were fused into one structure in areas of close apposition of the adjoining cells.

The presence of protein myozap in the plaques of cell-cell contact regions could be detected in both non-contracted and contracted states, the latter resulting in typical undulating surface profiles (compare, for example, Fig. 3f with Fig. 3g). Myozap also localized to plaque-coated adhesion structures in extended "free surface regions" facing the surrounding connective tissue compartment at the periphery of the smooth muscle cell bundle (Fig. 3a-c).

Transmission electron microscopy was performed to further characterize the extent and arrangement of the plaque-bearing plasma membrane regions in the smooth muscle cell bundles of bovine urinary bladder coats. Fig. 4 highlights the extent of the plaque-bearing regions. In cross section they appeared as ~0.3–1.0 μm domains (Fig. 4a, c; see also Fig. 3a-e) corresponding to the punctate anti-myozap immunofluorescence staining (Fig. 1a, b, b′, d, f). Conversely, longitudinal sections revealed strands that extended along most of the cellular surface (Fig. 4e-h), which has been referred to previously as rib-like arrays of dense plaques producing a rippled surface (Small and Gimona, 1998). The different degrees of crenulation correspond to different degress of contraction. Thus, the highly interdigitated junction-bearing cell borders in Figs. 3g and 4e, f, h signify cell contraction whereas the much straighter cell borders in Figs. 3f and 4g reflect a more relaxed state of contractility (see also (Gabella, 1976; Kelly and Rice, 1969)). These prominent strands of cytoplasmic plaque material correspond to strands detected in the anti-myozap immunofluorescence micrographs of longitudinal sections of bovine urinary bladder coat (Fig. 1c, c'). The intercellular space was marked by a single prominent electron-dense linear, partly granular structure in regions of close cell-cell apposition (40–70 nm) corresponding to the fused basement membranes of the adjacent cells (Fig. 4a-h). This is in line with the localization of collagen IV around individual smooth muscle cells (Fig. 1f' and Fig. S2b'). Local widening of the intercellular space occurred frequently, which was accompanied by duplication of the electron-dense lamina and occasional insertion of thick collagen fibrils (Fig. 4e, f; see also Fig. 3a-e). Plaque-bearing membrane domains were also readily detectable at connective tissue interfaces (Fig. 4h, i; see also Fig. 3a-c). All membrane-associated plaque ridges shared ultrastructural features. They had a fluffy electron-dense appearance and were in close apposition to the cytoplasmic actin filaments, which penetrated and inserted into the plaque material. Plaques protruded 25–40 nm into the cytoplasm. In rare instances, plaque-coated AJ-type puncta adhaerentia with a narrow (10–15 nm) extracellular interspace lacking the ECM middle lamella structure could be detected. They were typically positioned at the very end of long cell-cell adhesion regions (Fig. 4b, g).

The plaque-bearing membrane domains were interrupted by membrane regions with neighboring 40–60 nm vesicles in large numbers (brackets in Fig. 4a, c, e, g, h; see also Fig. 3b-e). Many of the vesicles were closely attached to or even fused with the plasma membrane forming flask-like caveolar structures that were arranged as long arrays similar to those encountered in endothelial cells (Stan, 2002). These regions lacked the dense actin filament mesh. At cell-ECM interfaces exosome-like structures were detected before and after budding (Fig. 4h,



(caption on next page)

Fig. 2. Myozap can be detected immunobiochemically in various tissues of the mammalian urogenital and gastrointestinal tract. The immunoblots using polyclonal guinea pig antibodies identify protein myozap in its isoelectric variants after 1D- and 2D-SDS-polyacrylamide gel electrophoresis in smooth muscle cell-enriched cytoskeletal fractions from various tissues. Apparent molecular weight (mol. wt.) values are indicated in kDa on the left margin. (a) The immunoblot reaction after 1D-SDS-PAGE shows a single major myozap band at a mol. wt. of ~54 kDa in muscle-enriched tissue material of human gallbladder, ureter, urinary bladder, urethra and ductus deferens. Note also the negative reaction in kidney included for control. (b) The corresponding myozap band is recognized in urinary bladder smooth muscle tissue preparations of human, bovine, porcine and murine (rat) origin. (c) Immunoblot of a 2D-gel electrophoretic separation of cytoskeletal proteins of smooth muscle tissue of human urinary bladder, showing the five major isoelectric variants of protein myozap (arrows) in comparison with the positions of the co-electrophoresed reference polypeptides bovine serum albumin (BSA; IEP: 6.4), phosphoglycerokinase (PGK; IEP: 7.4) and non-muscle actin (Actin; IEP: 5.4). (d) Parallel 2D-gel electrophoretic analysis showing the isoelectric variant pattern of myozap in a human heart tissue preparation. (e) Result of a 2D-gel electrophoresis of a mixture of near-equal amounts of proteins of both human tissues, urinary bladder wall and heart. Note that the two predominant isoelectric variants of the heart tissue sample (arrows in (d)) are identical to the two most basic ones of the five isoelectric variants identified in the preparation of bladder smooth muscle proteins (denoted by five arrows). The arrowhead in (d) denotes a further, very minor isoelectric variant of questional significance in heart tissue.

i).

3.4. Myozap shows widespread co-localization with plectin in smooth muscle cell junctions

Wiche et al. (1983) reported that antibodies directed against the cytolinker plectin show a staining pattern in rat urinary bladder that is very similar to that observed for anti-myozap antibodies (Fig. 1). Double immunofluorescence microscopy showed that myozap and plectin co-localize to a very large degree (Fig. 5). Both antigens exhibit an almost identical distribution pattern both in cross-section and longitudinal section. Co-localization was not only restricted to regions of cell-cell contact but was also noted at cell-ECM interfaces. We therefore conclude that myozap and plectin are both components of the plaque material subjacent to the junctional strands and that plectin may contribute to the anchorage of actin filaments.

3.5. Myozap-positive junctions alternate with caveolin- and dystrophin-rich membrane domains

It has been shown that plectin-positive strands alternate with caveolin- and dystrophin-enriched plasma membrane regions in smooth muscle cells of rat colon (Tanaka et al., 2001). To determine whether this is also the case in smooth muscle cells of the urinary tract and whether myozap is again involved, we performed double label immunofluorescence microscopy. Fig. 6a-c shows that caveolin antibodies revealed a patchy distribution. Detailed examination showed that caveolin and myozap localized in close proximity but did not show co-localization in regions of highest resolution. The observations are compatible with the electron microscopy images in Figs. 3, 4 showing alternating plasma membrane regions which are either rich in vesicles and caveolar structures or contain plaque-decorated junctional strands. The fluorescence micrographs furthermore showed that caveolin-staining was most prominent at cell-ECM contact sites. This was also supported by transmission electron microscopy, which showed the most extensive vesicular regions at the interface of smooth muscle cells with the ECM (Fig. 4h).

Double label immunofluorescence microscopy for dystrophin and myozap was slightly different from that observed for caveolin and myozap. Anti-dystrophin staining was much more evenly distributed throughout the smooth muscle cell bundles with only marginal if any labeling of contact regions between muscle cells and the ECM (Fig. 6d-g). In thin sections, anti-dystrophin and anti-myozap distribution could be clearly separated with alternating pattern (Fig. 6 f, g). We therefore conclude that dystrophin co-localizes with caveolin at the vesicle-rich plasma membrane domains and that these domains alternate with myozap-/plectin-rich regions. This is in full agreement with the previously proposed bipartite smooth muscle cell plasma membrane organization (North et al., 1993).

3.6. Myozap-positive junctions contain a select set of major focal adhesion proteins

That the myozap-positive ridges may share properties of focal adhesion plaques is suggested by their partial colocalization with – or very close correspondence – to α5 integrin (Fig. 7a; Fig. S3) as well as β1-integrin (Fig. 7b; Fig. S4), i.e. hallmark transmembrane proteins of focal adhesions. Immunolocalization results yet difficult to explain are those obtained for the tetraspan transmembrane protein CD151 which in some bundle regions localized very close to protein myozap and β1-integrin but was totally negative in other bundles or bundle regions (Fig. 7c; for other localizations of this molecule see (Sterk et al., 2000)).

In the next set of experiments, we analyzed the distribution of cytoplasmic focal adhesion components in relation to the myozap-positive strands (Fig. 7d-f). These analyses revealed similarities and differences. Thus, talin co-localized almost perfectly throughout with myozap (Fig. 7d; Fig. S5). Similarly, vinculin also co-localized with myozap, although to variable degrees, and was clearly different from dystrophin-positive regions (Fig. 7e, f; Figs. S6, S7).

Taken together, we find that the junctional myozap-positive junctional strands are a junction type sui generis, which, however, shares similarities with ECM-associated focal adhesions.

3.7. Myozap-positive junctions differ from adherens junctions

In extensive control experiments, using single- and double-label immunofluorescence microscopy, we examined the occurrence of constituent molecules of classical plaque-bearing cell-cell junctions in the rippled cell-cell adhesion structures. We found that the myozap, inter alia, positive plaque structures were consistently negative for the transmembrane molecules α6-integrin, HD230/233, N-, E-, and P-cadherin, cadherin−11, desmogleins 1–3, desmocollins 1–3 and PERP, as well as for the desmosomal and AJ plaque proteins desmoplakin, α-catenin, l/s-afadin, proteins ZO−1 and ZO−2 but also for the armadillo-type proteins β-catenin, plakoglobin, plakophilins 1–3 as well as proteins p120 and p0071 (for antibodies used see Table 1 and (Domke and Franke, 2019)). Only very rarely did we detect dot-like ZO−1, α- and β-catenin-positive structures at - mostly marginal - contact sites of some of these cells which were also positive for N-cadherin, cadherin-11, plakoglobin as well as for proteins p120 and p0071 and represented "normal" AJs of the puncta adhaerentia type (Fig. 8).

4. Discussion

In a systematic biochemical and multi-faceted histological study we have found that protein myozap (Seeger et al., 2010), which does not show amino acid sequence homologies to any other junctional plaque protein, is a major protein of the actin microfilament-anchoring plaques associated with conspicuous integrin-based focal adhesion-type structures arranged in ripple-like, usually very long plaque arrays characteristic of a major type of smooth muscle cell bundles. These myozap-positive, densely packed cells represent one of the most frequent smooth muscle cell types in the mammalian body where they

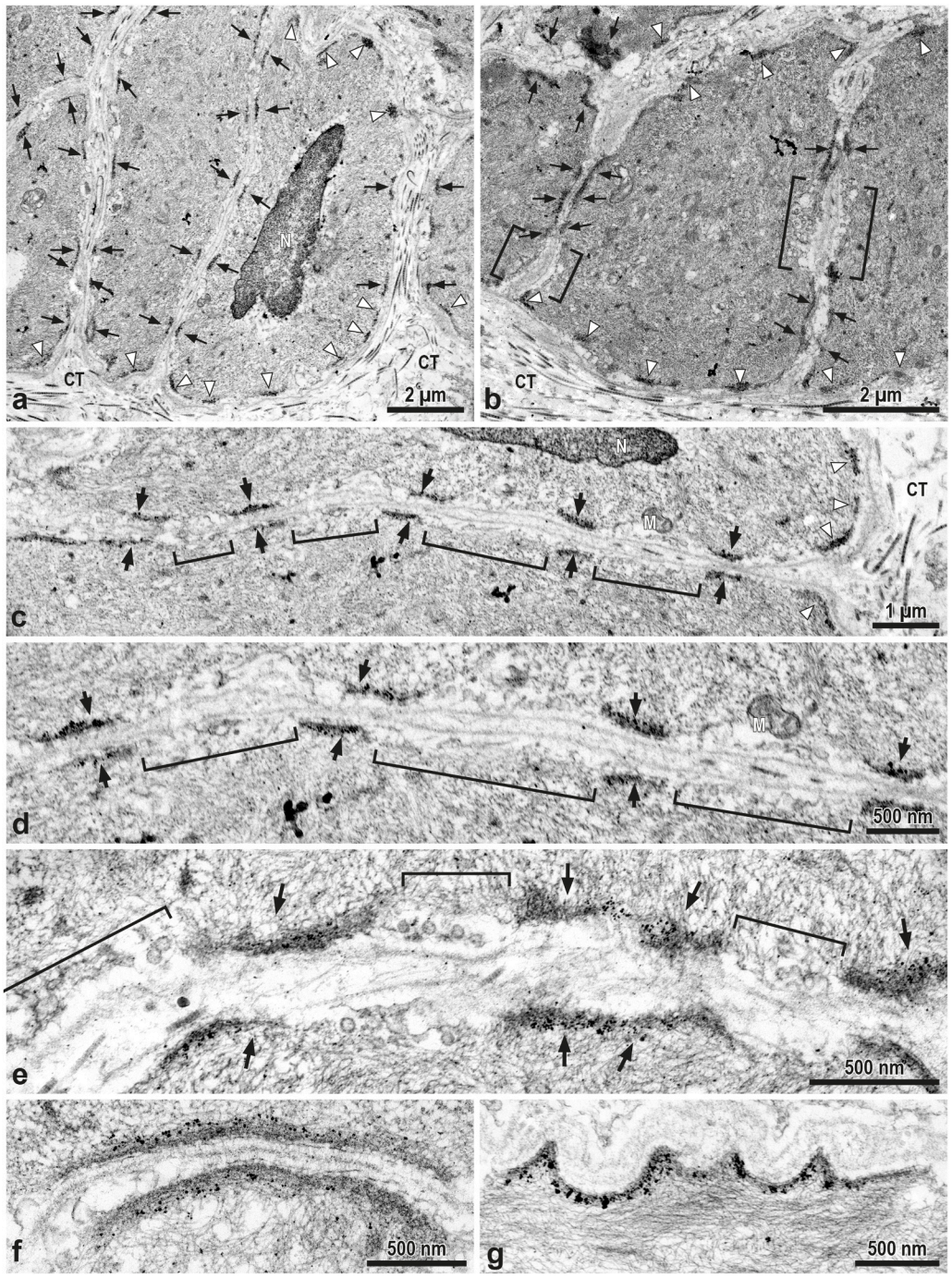


Fig. 3. Myozap is localized in cytoplasmic plaques at distinct plasma membrane regions of smooth muscle cells. The immunoelectron micrographs show cross sections (a-e) and near-longitudinal sections (f, g) through cytoplasmic plaque-covered plasma membrane regions of cell junctions of smooth muscle cells in bovine bladder muscular coat tissue after gold grain-labelled immunoreactions (silver enhancement) with murine monoclonal antibodies to protein myozap. (a, b) Immunoelectron micrographs through groups of cells located in the periphery of smooth muscle cell bundles. Cytoplasmic plaque-bearing plasma membrane regions are labelled by arrows at intercellular spaces and by arrowheads at cell-connective tissue borders. Note a few junction places in which cells are still in relatively close cell-cell junction contact in contrast to the rather large and wide separations of many corresponding cell-cell junctions by ECM structures including collagen fiber bundles. Note also the midline-equivalent ECM structures between these cells corresponding to the basement membranes of adjacent cells. Plaque-free regions with abundant small vesicles and reduced cytoplasmic actin are demarcated by brackets in (b). CT, connective tissue; N, nucleus. (c-g) Note that the anti-myozap immunogold marker particles label exclusively the electron-dense plaque structures. Corresponding plaques of the cell-cell junction pairs are labelled with arrows in (c-e), the intermittent plaque-free membrane regions are indicated by brackets in (c-e). (c, d) are taken from (a) depicting cell-cell contacts a higher magnification for better visualization of gold particles. Note the two lines which correspond to the basement membrane of the adjacent cells and separate the plaques of the adjoining cells. Also note the high membrane-attachment density of the plaque connections with actin-containing myofilaments (e-g). (f) Region with basement membrane and (g) example of a plasma membrane region in a contracted cell in which the plaque structures are continuous and labelled with immunogold. CT, connective tissue; N, nucleus; M, mitochondrium.

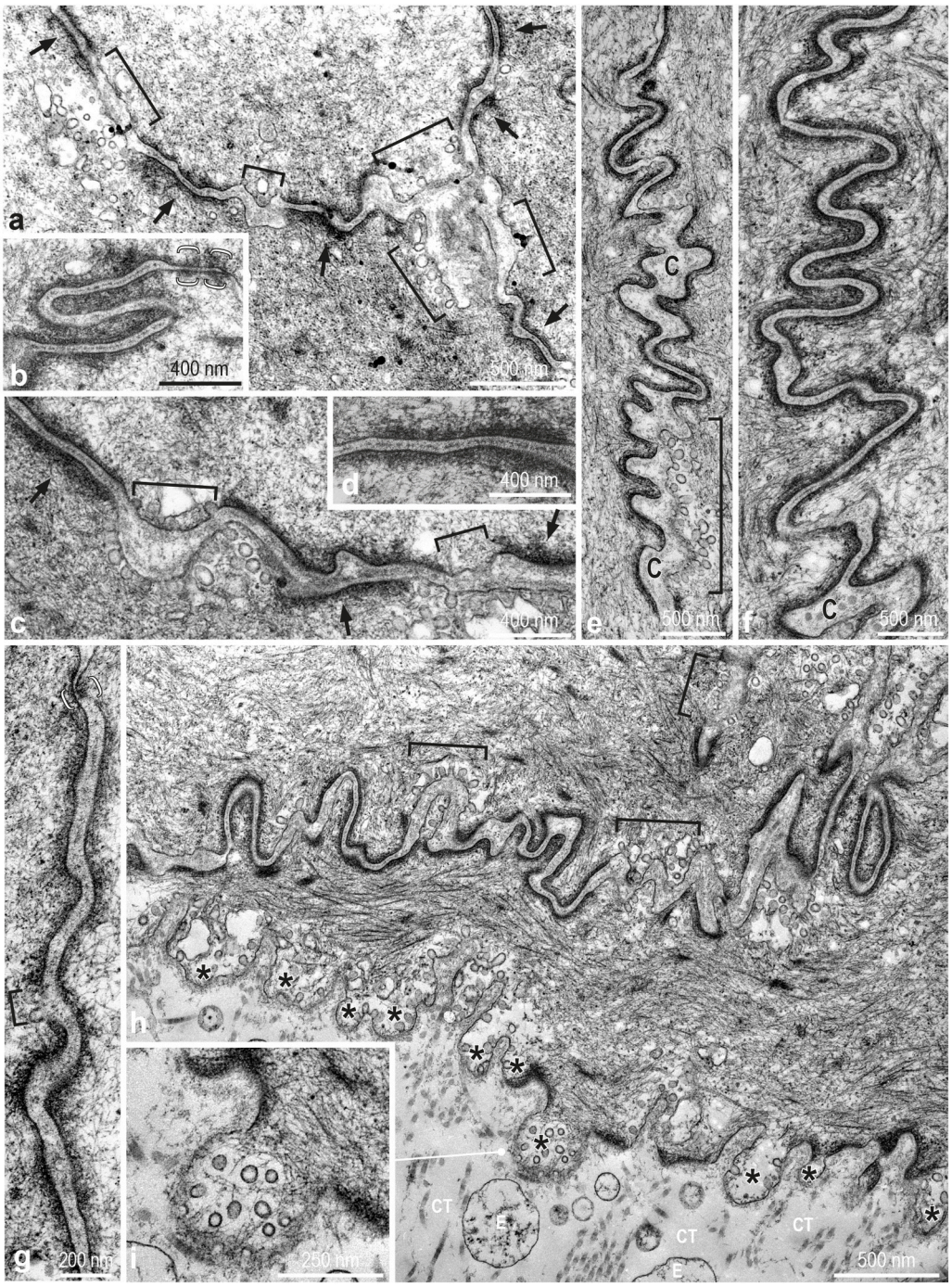


Fig. 4. Extensive regions of junction plaque ridges can be identified in electron micrographs of ultrathin cross and near-longitudinal sections in smooth muscle tissue of bovine urinary bladder coats. The transmission electron microscopy images show cell-cell junctions in cross sections (a-d) and near-longitudinal sections (e-h) as well as cell-ECM junctions (h, i). Note that in the cell-cell junction regions both plasma membranes are for the most part relatively closely associated (40–70 nm) and characterized by an - often very long and massive - electron-dense cytoplasmic plaque ridge (indicated by arrows in a and c). Dense material corresponding to basement membranes are often also revealed in the intercellular space. Larger-sized intercellular spaces contain special ECM structures, including collagen fibrils (e.g., structures labelled C in e, f). Note also that the cytoplasmic plaque structures are interrupted by specific membrane regions which contain caveolar membrane formations (e.g., denoted by black brackets in a, c and e) on one or - mostly - both of the two cell-cell connecting plasma membranes. Occasionally occurring puncta adhaerentia-type AJs at the end of plaque ridges are labeled by white brackets in (b) and (g). (h, i) Surface region of a smooth muscle cell bundle of a urinary bladder tissue coat of a fetal calf seen in an electron micrograph of a longitudinal section. Note that the outer cell (bottom) is connected to the inner cell (top) by a cell-cell contact junction structure of plaque ridges and interspersed caveolar regions (black brackets) whereas the plasma membrane of the outer cell facing the ECM contains some focal adhesion-like attachment plaques alternating with membrane-associated vesicular structures and small "free" membrane vesicles located in plasma membrane protrusions (asterisks; enlargement in **i**). These protrusions may bud off to form the membrane-coated structures observed nearby (E). CT, connective tissue.

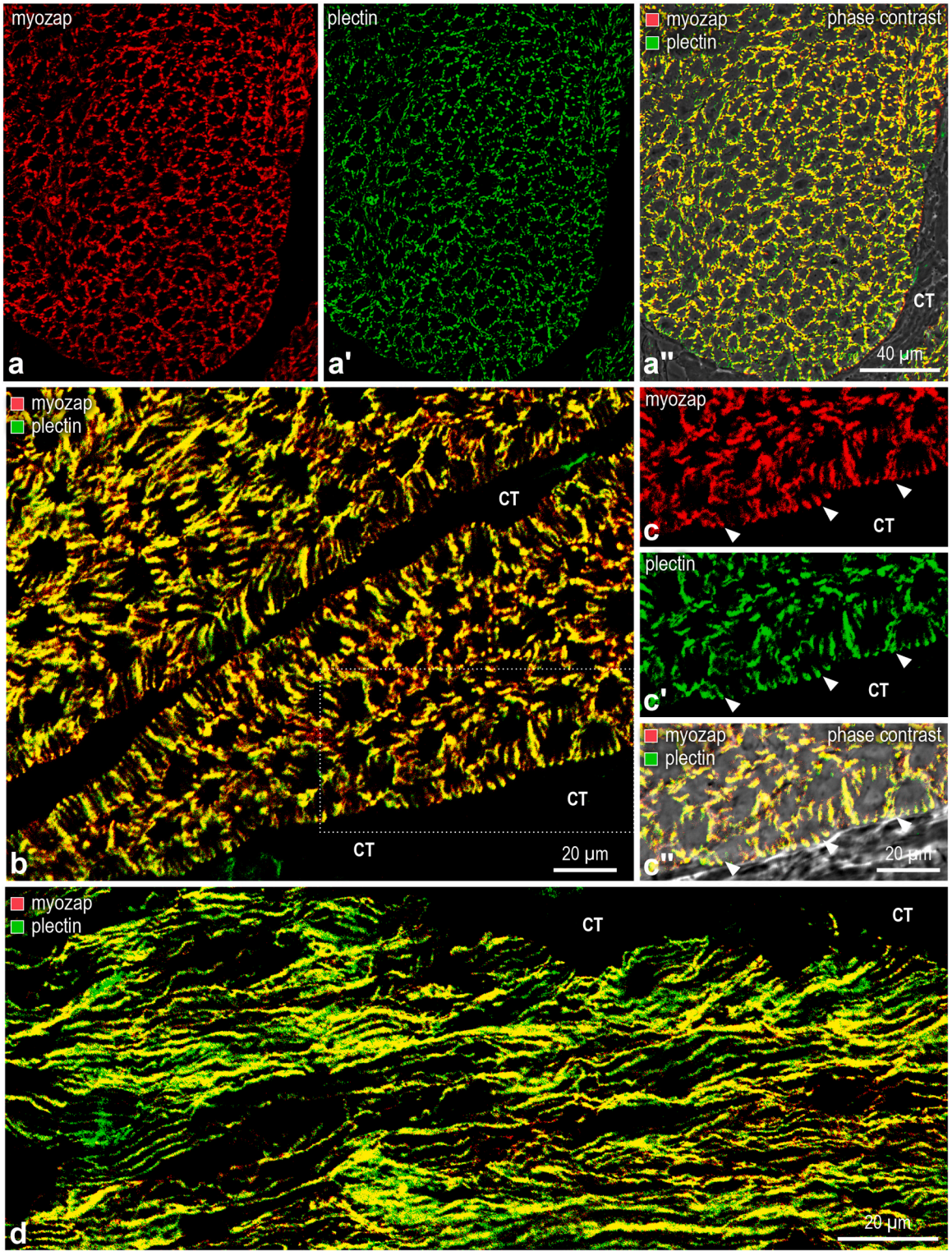


Fig. 5. Myozap co-localizes with plectin in muscularis coat of bovine urinary bladder. Immunofluorescence microscopy showing the colocalization of the proteins myozap (monoclonal murine antibody; red) and plectin (polyclonal guinea pig antibodies; green). Note the apparently punctate colocalization of both junction plaque proteins (yellow merger color) in cross sections through smooth muscle cell bundles (a–c") as well as their appearance in the closely parallel, very thin appearing junction plaque ridges ("ribs" sensu of V. Small) in near-longitudinal sections (d). The ECM borders are seen in overlaid phase contrast micrographs (a", c"). (b-c") High magnifications (boxed area in b at higher magnification in c-c") of - for the most part - cross-sections illustrate frequency, sizes and densities of the plasma membrane-associated myozap- and plectin-positive plaque ridge structures (yellow merger color) occurring at cell-cell junctions and the somewhat smaller plasma membrane plaque structures at the peripheral side of the outer cells along the muscle bundle peripheries (arrowheads), presumably corresponding to the attachment plaques shown in Figs. 3a, b and 4h. (c"). CT, connective tissue.

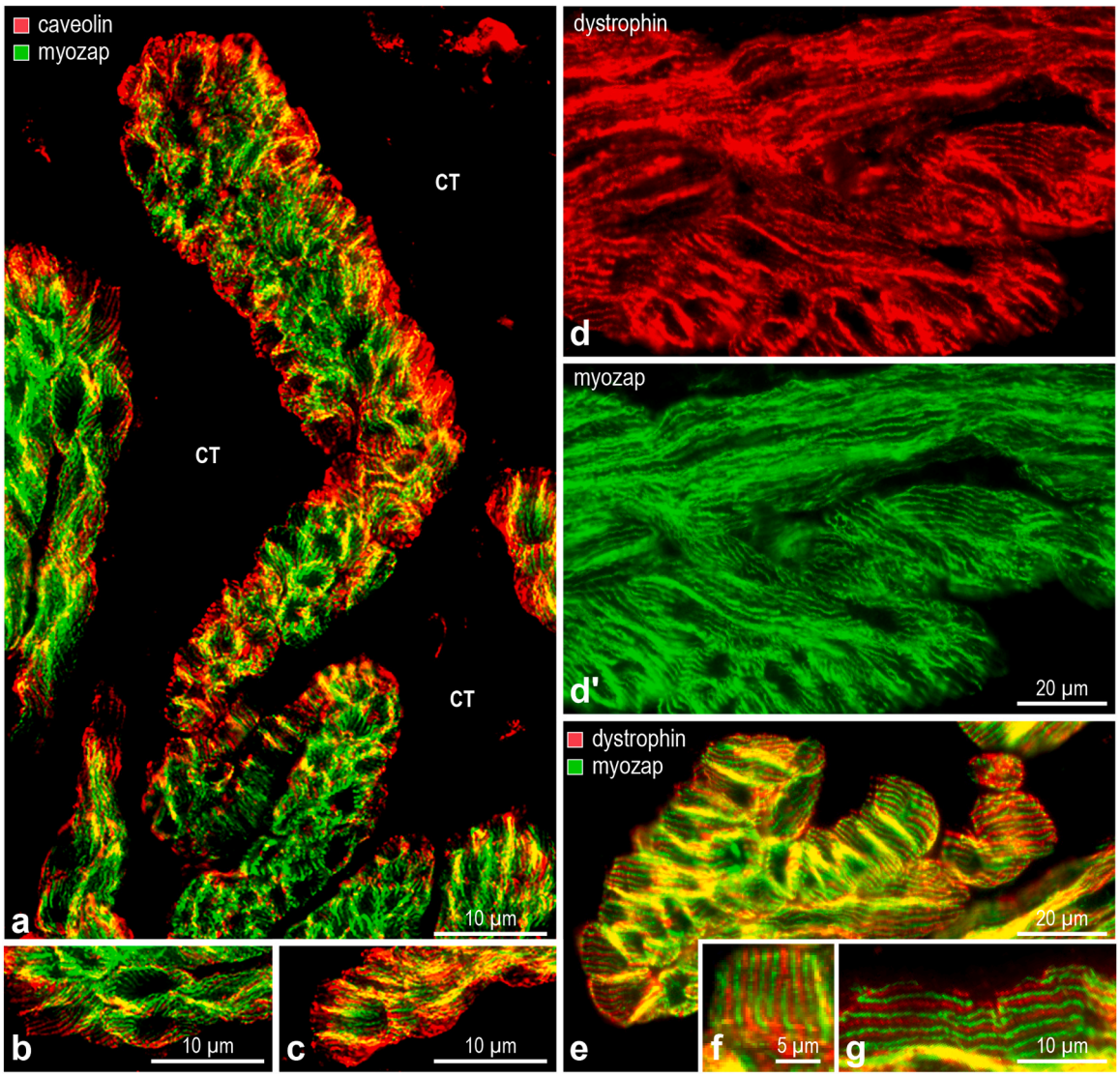


Fig. 6. Myozap-positive regions alternate with caveolin- and dystrophin-positive regions. (a) Immunofluorescence micrograph of a cross section through bundles of smooth muscle muscular coat tissue of snap-frozen bovine urinary bladder, showing here the abundance of caveolin-rich plasma membrane regions (red; monoclonal rabbit antibodies) at the muscle bundle cell surfaces as well as partially in association with the protein myozap-positive (polyclonal guinea pig antibodies; green) plasma membrane-associated attachment plaques. The anti-caveolin reaction in the connective tissue (CT) compartment is due to staining of vascular walls. (b, c) illustrate details of mostly non-overlapping anti-caveolin and anti-myozap immuoreactions. (d, d′) Double-label immunofluorescence survey micrographs showing longitudinal sections of smooth muscle tissue bundles of bovine urinary bladder coat after reactions with rabbit antibodies to dystrophin (d) and guinea pig antibodies to protein myozap (d′). Note closely parallel-associated, very thin paths covered with dystrophin-positive (red) structures or with myozap-positive (green) structures. Many of these very thin and closely spaced structures appear in yellow merger color (not shown). Obviously, a major part of the lateral smooth muscle cell-cell contact regions is occupied by these two forms of plasma membrane junctions. (e-g) High resolution revealing very thin and narrow-spaced cell-cell junction plaque cords stained positive for protein myozap (green; polyclonal guinea pig antibodies) in lateral alternations with very narrow dystrophin-positive lanes (red; polyclonal rabbit antibodies). Note that these two closely parallel plasma membrane associated cell-cell junction structures occupy almost the entire cell-cell contact plasma membrane junction area. Both the myozap-containing (green-stained) junction plaque cord structures and the closely adjacent dystrophin-positive lanes (red-stained) are only 300–450 nm broad. Note also that in some places the two kinds of longitudinal structures are very closely associated and partly overlapping, resulting in the appearance of yellow merger color.

occur as predominantly outer, mostly longitudinal bundles in the urogenital, the alimentary and the airway tracts.

The cell adhesion structures with the myozap-rich plaques described here, whether completely or incompletely symmetrical, directly involved in cell-cell attachment or dissociated, are neither structurally nor compositionally related to the known families of cell-cell junction structures, including e.g., the zonulae or fasciae adhaerentes, the puncta adhaerentia, or the areae compositae of the cardiac intercalated disc (although the latter also contain myozap). They are, however, not at all restricted to the urinary tract but also connect the smooth muscle cells of the outer bundles accompanying large portions of the visceral tract, notably the esophagus, the stomach, all intercepts of the intestine as well as the gall bladder and bile ducts (e.g., (MacPherson et al., 1984)) although the molecular composition has not been determined comprehensively so far. It furthermore remains to be investigated whether and where comparable myozap-positive structures occur in the female genital tract, especially in the myometrium. Furthermore, distribution in tumors has not been explored.

These "focal adhesion"-type structures with their prominent dense plaque coats so abundant and prominent in the smooth muscle cell bundles of the muscle coats of the urinary bladder as well as other intercepts of the urogenital tract such as the ureter, the urethra, and the

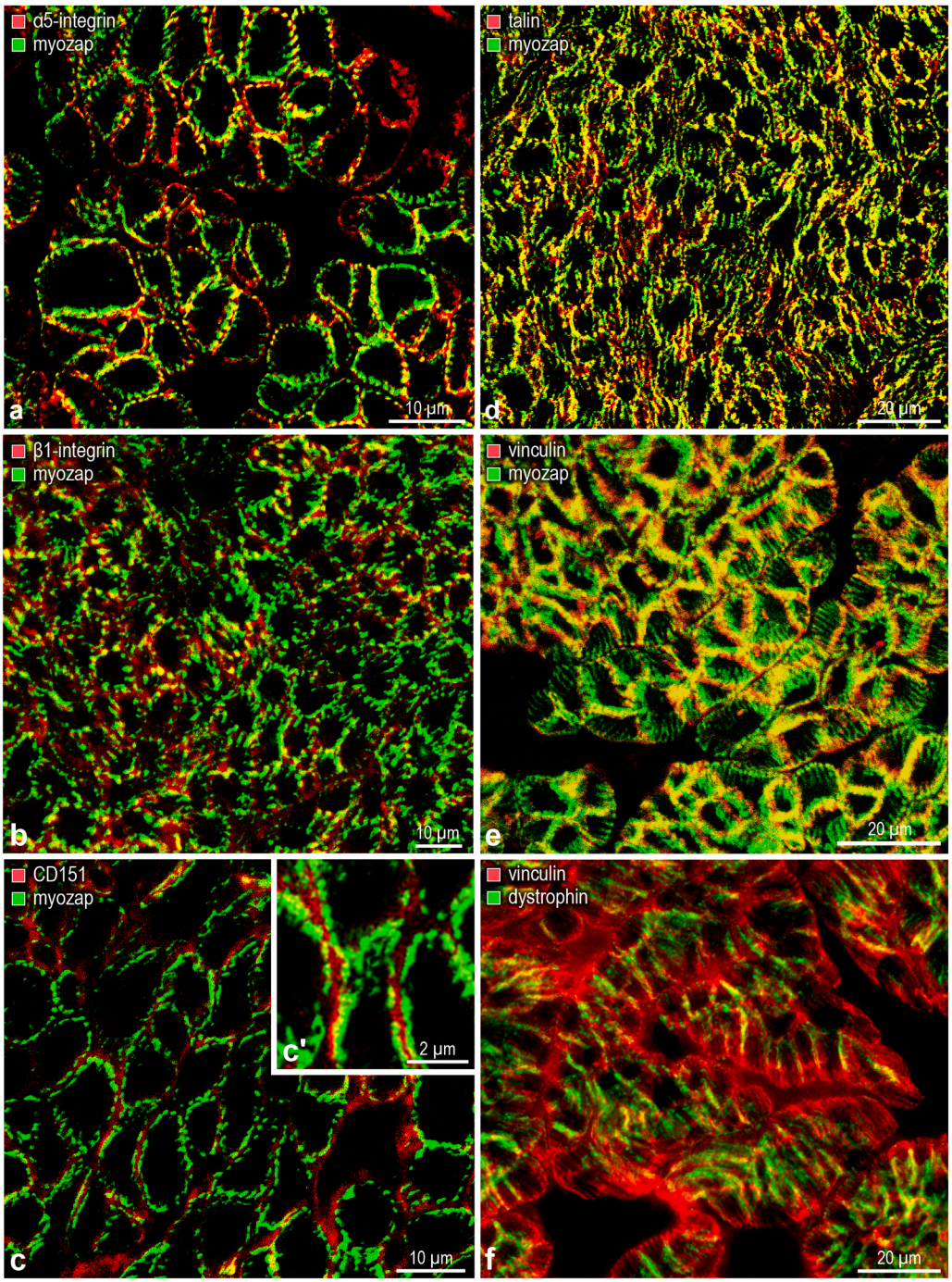


Fig. 7. Myozap co-localizes to different degrees with some focal adhesion proteins. The images show double-label immunofluorescence reaction micrographs of sections through smooth muscle tissue bundles of snap-frozen human (a, b, d-f) and bovine (c) bladder muscular walls. Note that the cytoplasmic plaque protein myozap (guinea pig antibodies; green) is closely associated with the major focal adhesion transmembrane glycoproteins α5-integrin/CD49e (a; murine monoclonal antibodies; red) and β1-integrin (b; rat monoclonal antibodies; red). Double label immunofluorescence in (c) and (c' detects co-localization of myozap (guinea pig antibodies; green) and the tetraspanin CD151 (mouse monoclonal antibodies; red) in some regions. A close correlation is observed for myozap (guinea pig antibodies; green) and the cytoplasmic plaque proteins talin (d; mouse monoclonal antibodies; red) and vinculin (e; mouse monoclonal antibodies; red). (f) The double-label immunofluorescence micrograph of a cryostat section shows the distribution of vinculin (mouse monoclonal antibody; red) and dystrophin (rabbit polyclonal antibodies; green). Note their differential distribution patterns. Further details are presented in Figs. S3–7.

seminal vesicle obviously play important roles in urine accumulation and let-down. Not surprisingly, such structures have been repeatedly described by previous authors but neither the principles of their cell and molecular biological organization nor their specific functions have been correctly and satisfactorily recognized. Practially, in all earlier reports these structures have been interpreted as a histologically specific variant of punctum adhaerens-type AJ (for reviews see, e.g., (McCloskey, 2010, 2011; Rasmussen et al., 2009). Apparently, the cadherin- and catenin-positive cells identified by the authors mentioned are interspersed "interstitial cells" ("Cajal cells") of the bladder. Our present work demonstrates that these prominent junctional structures of smooth muscle cells represent a novel cell biological type of cell-cell junction differing fundamentally from AJs but rather being related to – albeit not identical with – focal adhesions. In striking contrast to other cell-cell

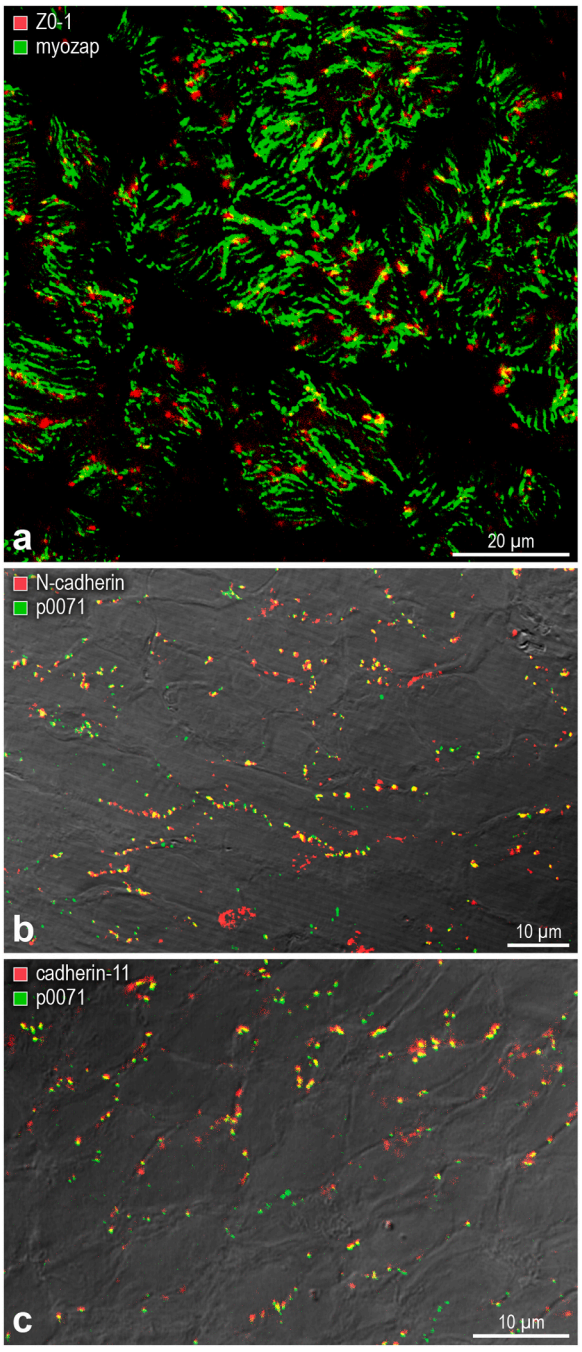


Fig. 8. Myozap does not co-distribute with adherens junction proteins. (a) Double-label immunofluorescence microscopy of a cryostat section through a cell-cell junction-rich plasma membrane region of bovine bladder muscular wall. Note the very different patterns of the typical small puncta adhaerentia junctions, recognized here as positively stained with murine monoclonal antibodies to protein ZO−1 (red), which sometimes appear in yellow merger color where they are located in close vicinity of - or optically overlapping with - protein myozap-containing cytoplasmic plaque cords (green; immunostaining with polyclonal guinea pig antibodies). (b, c) Rather small N-cadherin- or cadherin-11-based cell-cell junctions (b, N-cadherin, red; c, cadherin−11, red; both detected with monoclonal murine antibodies) of the puncta adhaerentia type are detected on a phase contrast background in bovine bladder muscular walls, often forming complexes with corresponding cytoplasmic plaque proteins of the cadherin-junction / AJ type, here with protein p0071 (b, c; green; polyclonal guinea pig antibodies). These AJ structures are fundamentally different from the cell-cell junctions characterized by protein myozap-containing plasma membrane plaque ridges of the elongated, extended smooth muscle cell-cell junctions.

junctions, the myozap-rich smooth muscle cell junctions are not based on direct transcellular contacts of transmembrane proteins or surface glycoproteins but represent extensive plasma membrane regions coated with cytoplasmic plaque ridges.

Certainly misleading has also been – and still is – the classification of these smooth muscle cells as "striated muscle fibers", a term introduced for and occupied by the cross-striated skeletal and cardiac sarcomeric muscle fibers. However, as clearly has been demonstrated in the present article, the "striations" in the mononuclear smooth muscle cells under question here are longitudinal structures representing the parallel ripples of the focal adhesion plaques (for an example of true "cross-striation" in the sense of the sarcomeric structures in certain urethric smooth muscles see (Dixon and Gosling, 1977).

Forces generated by the cytoplasmic actomyosin system must be transferred to neighbouring cells and the ECM to elicit coordinated smooth muscle cell bundle contraction enabling processes such as peristalsis of the ureter and intestine or voiding of the urinary bladder. The specificity and consistency of myozap localization throughout all dense plaques of the abundant junctional strands in major smooth muscle cell bundles of these organs argues for a central function of this still poorly characterized protein in force transmission. Recent publications provide evidence that in the heart muscle myozap is involved in mechanosensation and mechanotransduction (Borlepawar et al., 2020; Frank et al., 2014; Kluge et al., 2019; Rangrez et al., 2013, 2016), which is enabled by its central position in the force transmission chain. Junctional arrangement, however, differs fundamentally between cardiomyocytes and smooth muscle cells. While intercalated discs are perpendicular to the main cell axis, the junctional strands are lateral to the main axis of smooth muscle cells. Given the differences in the arrangement of the contractile actomyosin system, however, either junction type may still be aligned perpendicular to the main forces in both situations. It is tempting to speculate that myozap may contribute to the organization or stabilization of mechanically active interfaces in both cell types.

At the molecular level, myozap is associated with a specific ensemble of cytoplasmic proteins (notably plectin, talin and vinculin), which connect junctions to the actin cytoskeleton (recent reviews in (Geiger et al., 2023; Goult et al., 2018; Outla et al., 2025; Zhao et al., 2022)). The identification of the Rho-family GTPase 1 (Rnd1) as an interaction partner of myozap (Kluge et al., 2019) assigns a function in mechanosensation. Myozap is furthermore linked to transmembrane proteins (integrins, tetraspanins). Remarkably, the linkage extends beyond cell borders as evidenced by the recruitment of specific ECM components next to the smooth muscle cell junctional strands. Thus, Tanaka et al. (2001) reported that β2-chain laminin exclusively co-localized with plectin whereas β1-chain laminin stained the entire basement membrane in smooth muscle cells of rat colon. Similarly, North et al. (1993) detected co-distribution of fibronectin and vinculin.

Taken together, the data presented in this paper assign myozap an important juxtamembraneous position within the mechanical framework of smooth muscle cells. The myozap-positive membrane domains are maintained irrespective of the contraction status (see also (Small, 1985)). They alternate with more plastic dystrophin-containing plasma membrane domains that are rich in caveolar structures, which are known to be involved in mechanotransduction (e.g., (Brooks et al., 2023; Osmani et al., 2018; Sotodosos-Alonso et al., 2023)) and may change in size to accommodate the drastic cell shape changes that occur during smooth muscle cell bundle contraction. The scheme in Fig. 9 summarizes our current view of the alternating surface domains in the relaxed and contracted state. The stable myozap-positive junctional strands are functionally coupled across cell borders transducing mechanical forces between adjacent cells. They wrinkle during contraction forming interdigitating ripples. The interspersed plaque-free membrane regions, on the other hand, are highly dynamic, accommodating membrane remodelling by forming invaginations and vesicles that are rich in caveolin to support cycles of surface reduction and expansion during

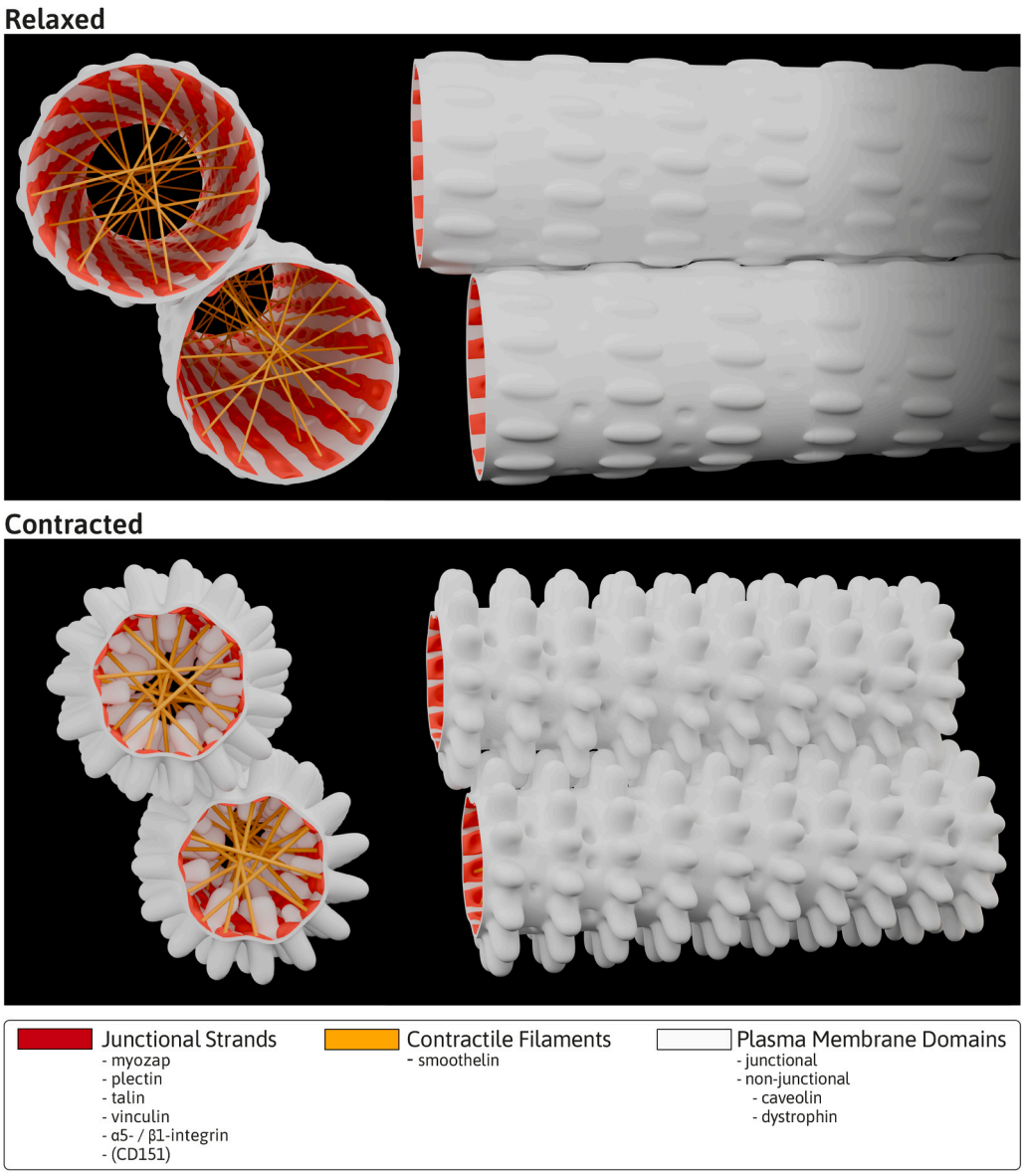


Fig. 9. 3D model of relaxed and contracted smooth muscle cells. The scheme depicts segments of two muscle cells (cross section at left; surface view at right) that are attached to each other by longitudinal myozap-positive junctional strands (red). The junctional strands are decorated by cytoplasmic plaque material that is connected to the intracellular contractile apparatus (rods). Note that the junctional strands wrinkle upon acto-myosin contraction forming intercalated ripples. The scheme also highlights subplasmalemmal vesicles in association with the junction-free membrane regions. They are positive for caveolin and increase in number during contraction to compensate for the reduced surface. Corresponding Video 1 presents an animation of the contractile cycle illustrating the dynamic aspects of junctional wrinkling and interjunctional vesicle formation. Listed at the bottom are only the polypeptides whose distribution was analysed in the present study by immunohistology.

smooth muscle cell contraction and relaxation.

CRediT authorship contribution statement

Roland Moll: Writing – review & editing, Formal analysis, Data curation, Conceptualization. **Adam Breitscheidel:** Visualization, Data curation. **Rudolf E. Leube:** Writing – review & editing, Visualization, Formal analysis, Data curation, Conceptualization. **Steffen Rickelt:** Investigation. **Franke Werner W:** Writing – original draft, Visualization, Supervision, Resources, Project administration, Investigation, Formal analysis, Data curation, Conceptualization. **Caecilia Kuhn:** Investigation. **Yvette Dörflinger:** Investigation. **Ralf Zimbelmann:** Investigation, Data curation. **Stefanie Winter-Simanowski:** Investigation.

Funding

This work was supported by the Federal Ministry for Research and Technology (WWF: BMBF; START-MSC; grant: 01GN0942).

Declaration of Competing Interest

The authors declare that they have no known competing financial interests or personal relationships that could have appeared to influence the work reported in this paper.

Acknowledgements

We thank Eva Gundel for organizational and editorial support throughout the project.

Appendix A. Supporting information

Supplementary data associated with this article can be found in the online version at doi:10.1016/j.ejcb.2026.151546.

Data availability

Data will be made available on request.

References

Borlepawar, A., Schmiedel, N., Eden, M., Christen, L., Rosskopf, A., Frank, D., Lullmann-Rauch, R., Frey, N., Rangrez, A.Y., 2020. Dysbindin deficiency Alters Cardiac BLOC-1 Complex and Myozap Levels in Mice. Cells 9. https://doi.org/10.3390/cells9112390.

Borrmann, C.M., Grund, C., Kuhn, C., Hofmann, I., Pieperhoff, S., Franke, W.W., 2006. The area composita of adhering junctions connecting heart muscle cells of vertebrates. II. Colocalizations of desmosomal and fascia adhaerens molecules in the intercalated disk. Eur. J. Cell. Biol. 85, 469–485. https://doi.org/10.1016/j.ejcb.2006.02.009.

Brooks, J.W., Tillu, V., Eckert, J., Verma, S., Collins, B.M., Parton, R.G., Yap, A.S., 2023. Caveola mechanotransduction reinforces the cortical cytoskeleton to promote epithelial resilience. Mol. Biol. Cell. 34, ar120. https://doi.org/10.1091/mbc.E23-05-0163.

Dixon, J.S., Gosling, J.A., 1977. Light and electron microscopic observations on noradrenergic nerves and striated muscle cells of the guinea pig urethra. Am. J. Anat. 149, 121–126. https://doi.org/10.1002/aja.1001490110.

Domke, L.M., Franke, W.W., 2019. The cell-cell junctions of mammalian testes: II. The lamellar smooth muscle monolayer cells of the peritubular wall are laterally connected by vertical adherens junctions-a novel architectonic cell-cell junction system. Cell. Tissue Res. 375, 451–482. https://doi.org/10.1007/s00441-018-2968-x.

Farquhar, M.G., Palade, G.E., 1963. Junctional complexes in various epithelia. J. Cell. Biol. 17, 375–412. https://doi.org/10.1083/jcb.17.2.375.

Frank, D., Rangrez, A.Y., Poyanmehr, R., Seeger, T.S., Kuhn, C., Eden, M., Stiebeling, K., Bernt, A., Grund, C., Franke, W.W., Frey, N., 2014. Mice with cardiac-restricted overexpression of Myozap are sensitized to biomechanical stress and develop a protein-aggregate-associated cardiomyopathy. J. Mol. Cell. Cardiol. 72, 196–207. https://doi.org/10.1016/j.yjmcc.2014.03.016.

Franke, W.W., 2009. Discovering the molecular components of intercellular junctions–a historical view. Cold Spring Harb. Perspect. Biol. 1, a003061. https://doi.org/10.1101/cshperspect.a003061.

Franke, W.W., Borrmann, C.M., Grund, C., Pieperhoff, S., 2006. The area composita of adhering junctions connecting heart muscle cells of vertebrates. I. Molecular definition in intercalated disks of cardiomyocytes by immunoelectron microscopy of desmosomal proteins. Eur. J. Cell. Biol. 85, 69–82. https://doi.org/10.1016/j.ejcb.2005.11.003.

Franke, W.W., Rickelt, S., 2011. Mesenchymal-epithelial transitions: spontaneous and cumulative syntheses of epithelial marker molecules and their assemblies to novel cell junctions connecting human hematopoietic tumor cells to carcinomatoid tissue structures. Int. J. Cancer 129, 2588–2599. https://doi.org/10.1002/ijc.26227.

Gabella, G., 1976. Structural changes in smooth muscle cells during isotonic contraction. Cell. Tissue Res. 170, 187–201. https://doi.org/10.1007/BF00224298.

Geiger, B., Boujemaa-Paterski, R., Winograd-Katz, S.E., Balan Venghateri, J., Chung, W. L., Medalia, O., 2023. The actin network interfacing diverse integrin-mediated adhesions. Biomolecules 13. https://doi.org/10.3390/biom13020294.

Goodenough, D.A., Paul, D.L., 2009. Gap junctions. Cold Spring Harb. Perspect. Biol. 1, a002576. https://doi.org/10.1101/cshperspect.a002576.

Goult, B.T., Yan, J., Schwartz, M.A., 2018. Talin as a mechanosensitive signaling hub. J. Cell. Biol. 217, 3776–3784. https://doi.org/10.1083/jcb.201808061.

Kelly, R.E., Rice, R.V., 1969. Ultrastructural studies on the contractile mechanism of smooth muscle. J. Cell. Biol. 42, 683–694. https://doi.org/10.1083/jcb.42.3.683.

Kluge, A., Rangrez, A.Y., Kilian, L.S., Pott, J., Bernt, A., Frauen, R., Rohrbeck, A., Frey, N., Frank, D., 2019. Rho-family GTPase 1 (Rnd1) is a biomechanical stress-sensitive activator of cardiomyocyte hypertrophy. J. Mol. Cell. Cardiol. 129, 130–143. https://doi.org/10.1016/j.yjmcc.2019.01.028.

Langbein, L., Pape, U.F., Grund, C., Kuhn, C., Praetzel, S., Moll, I., Moll, R., Franke, W. W., 2003. Tight junction-related structures in the absence of a lumen: occludin, claudins and tight junction plaque proteins in densely packed cell formations of stratified epithelia and squamous cell carcinomas. Eur. J. Cell. Biol. 82, 385–400. https://doi.org/10.1078/0171-9335-00330.

MacPherson, B.R., Scott, G.W., Chansouria, J.P., Fisher, A.W., 1984. The muscle layer of the canine gallbladder and cystic duct. Acta Anat. (Basel) 120, 117–122. https://doi.org/10.1159/000145904.

McCloskey, K.D., 2010. Interstitial cells in the urinary bladder–localization and function. Neurourol. Urodyn. 29, 82–87. https://doi.org/10.1002/nau.20739.

McCloskey, K.D., 2011. Interstitial cells of Cajal in the urinary tract. Handb. Exp. Pharmacol. 233–254. https://doi.org/10.1007/978-3-642-16499-6_11.

North, A.J., Galazkiewicz, B., Byers, T.J., Glenney Jr., J.R., Small, J.V., 1993. Complementary distributions of vinculin and dystrophin define two distinct sarcolemma domains in smooth muscle. J. Cell. Biol. 120, 1159–1167. https://doi.org/10.1083/jcb.120.5.1159.

Osmani, N., Pontabry, J., Comelles, J., Fekonja, N., Goetz, J.G., Riveline, D., Georges-Labouesse, E., Labouesse, M., 2018. An Arf6- and caveolae-dependent pathway links hemidesmosome remodeling and mechanoresponse. Mol. Biol. Cell. 29, 435–451. https://doi.org/10.1091/mbc.E17-06-0356.

Outla, Z., Prechova, M., Korelova, K., Gemperle, J., Gregor, M., 2025. Mechanics of cell sheets: plectin as an integrator of cytoskeletal networks. Open. Biol. 15, 240208. https://doi.org/10.1098/rsob.240208.

Pieperhoff, S., Rickelt, S., Heid, H., Claycomb, W.C., Zimbelmann, R., Kuhn, C., Winter-Simanowski, S., Kuhn, C., Frey, N., Franke, W.W., 2012. The plaque protein myozap identified as a novel major component of adhering junctions in endothelia of the blood and the lymph vascular systems. J. Cell. Mol. Med. 16, 1709–1719. https://doi.org/10.1111/j.1582-4934.2011.01463.x.

Rangrez, A.Y., Bernt, A., Poyanmehr, R., Harazin, V., Boomgaarden, I., Kuhn, C., Rohrbeck, A., Frank, D., Frey, N., 2013. Dysbindin is a potent inducer of RhoA-SRF-mediated cardiomyocyte hypertrophy. J. Cell. Biol. 203, 643–656. https://doi.org/10.1083/jcb.201303052.

Rangrez, A.Y., Eden, M., Poyanmehr, R., Kuhn, C., Stiebeling, K., Dierck, F., Bernt, A., Lullmann-Rauch, R., Weiler, H., Kirchof, P., Frank, D., Frey, N., 2016. Myozap deficiency promotes adverse cardiac remodeling via differential regulation of mitogen-activated protein kinase/serum-response factor and beta-catenin/GSK-3beta protein signaling. J. Biol. Chem. 291, 4128–4143. https://doi.org/10.1074/jbc.M115.689620.

Rasmussen, H., Rumessen, J.J., Hansen, A., Smedts, F., Horn, T., 2009. Ultrastructure of Cajal-like interstitial cells in the human detrusor. Cell. Tissue Res. 335, 517–527. https://doi.org/10.1007/s00441-008-0736-z.

Rickelt, S., Kuhn, C., Winter-Simanowski, S., Zimbelmann, R., Frey, N., Franke, W.W., 2011. Protein myozap–a late addition to the molecular ensembles of various kinds of adherens junctions. Cell. Tissue Res. 346, 347–359. https://doi.org/10.1007/s00441-011-1281-8.

Rickelt, S., Rizzo, S., Doerflinger, Y., Zentgraf, H., Basso, C., Gerosa, G., Thiene, G., Moll, R., Franke, W.W., 2010. A novel kind of tumor type-characteristic junction: plakophilin-2 as a major protein of adherens junctions in cardiac myxomata. Mod. Pathol. 23, 1429–1437. https://doi.org/10.1038/modpathol.2010.138.

Rickelt, S., Winter-Simanowski, S., Noffz, E., Kuhn, C., Franke, W.W., 2009. Upregulation of plakophilin-2 and its acquisition to adherens junctions identifies a novel molecular ensemble of cell-cell-attachment characteristic for transformed mesenchymal cells. Int. J. Cancer 125, 2036–2048. https://doi.org/10.1002/ijc.24552.

Schulzke, J.D., Gunzel, D., John, L.J., Fromm, M., 2012. Perspectives on tight junction research. Ann. N. Y Acad. Sci. 1257, 1–19. https://doi.org/10.1111/j.1749-6632.2012.06485.x.

Seeger, T.S., Frank, D., Rohr, C., Will, R., Just, S., Grund, C., Lyon, R., Luedde, M., Koegl, M., Sheikh, F., Rottbauer, W., Franke, W.W., Katus, H.A., Olson, E.N., Frey, N., 2010. Myozap, a novel intercalated disc protein, activates serum response factor-dependent signaling and is required to maintain cardiac function in vivo. Circ. Res. 106, 880–890. https://doi.org/10.1161/CIRCRESAHA.109.213256.

Small, J.V., 1985. Geometry of actin-membrane attachments in the smooth muscle cell: the localisations of vinculin and alpha-actinin. EMBO J. 4, 45–49. https://doi.org/10.1002/j.1460-2075.1985.tb02315.x.

Small, J.V., Gimona, M., 1998. The cytoskeleton of the vertebrate smooth muscle cell. Acta Physiol. Scand. 164, 341–348. https://doi.org/10.1046/j.1365-201X.1998.00441.x.

Sotodosos-Alonso, L., Pulgarin-Alfaro, M., Del Pozo, M.A., 2023. Caveolae mechanotransduction at the interface between cytoskeleton and extracellular matrix. Cells 12. https://doi.org/10.3390/cells12060942.

Stan, R.V., 2002. Structure and function of endothelial caveolae. Microsc. Res. Tech. 57, 350–364. https://doi.org/10.1002/jemt.10089.

Sterk, P., Kasperk, R., Opitz, T., Schubert, F., Klein, P., 2000. Vascular organization in the mesorectum: angiography of rectal resection specimens. Int. J. Colorectal Dis. 15, 225–228. https://doi.org/10.1007/s003840000237.

Straub, B.K., Rickelt, S., Zimbelmann, R., Grund, C., Kuhn, C., Iken, M., Ott, M., Schirmacher, P., Franke, W.W., 2011. E-N-cadherin heterodimers define novel adherens junctions connecting endoderm-derived cells. J. Cell. Biol. 195, 873–887. https://doi.org/10.1083/jcb.201106023.

Tanaka, H., Hijikata, T., Murakami, T., Fujimaki, N., Ishikawa, H., 2001. Localization of plectin and other related proteins along the sarcolemma in smooth muscle cells of rat colon. Cell. Struct. Funct. 26, 61–70. https://doi.org/10.1247/csf.26.61.

Wiche, G., Krepler, R., Artlieb, U., Pytela, R., Denk, H., 1983. Occurrence and immunolocalization of plectin in tissues. J. Cell. Biol. 97, 887–901. https://doi.org/10.1083/jcb.97.3.887.

Zhao, Y., Lykov, N., Tzeng, C., 2022. Talin-1 interaction network in cellular mechanotransduction (Review). Int. J. Mol. Med. 49. https://doi.org/10.3892/ijmm.2022.5116.

Supplementary Data

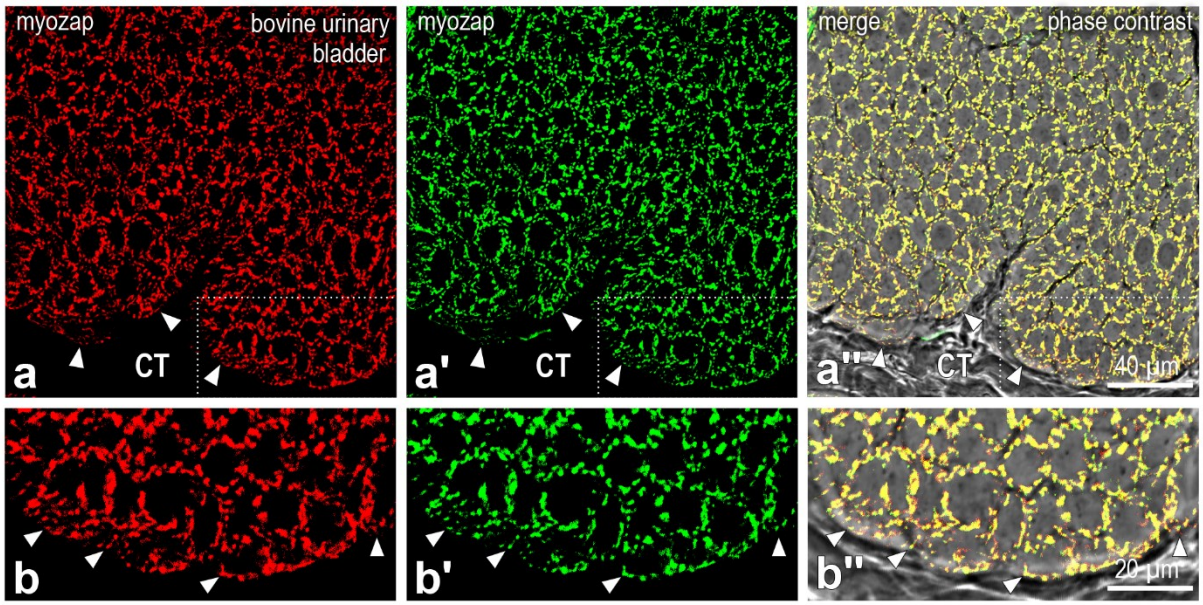


Fig. S1. Myozap localizes at cell-cell and cell-extracellular matrix interfaces in smooth muscle cells in the bovine urinary bladder. (see corresponding low magnification images in Fig. 1b, b')

Double-label immunofluorescence microscopy of a cryostat cross section through snap-frozen smooth muscle tissue of bovine urinary bladder muscularis coat using a murine monoclonal antibody to protein myozap (**a**; red) and polyclonal guinea pig myozap antibodies (**a'**; green) that are directed to different myozap epitopes. (**a''**) shows an overlay of (**a**) and (**a'**) together with the corresponding phase contrast recording. Regions demarcated by broken lines are shown at higher magnification in (**b-b''**). Note the colocalization of both immunoreactivities at cell-cell borders and at contact zones to the surrounding connective tissue (CT; arrowheads).

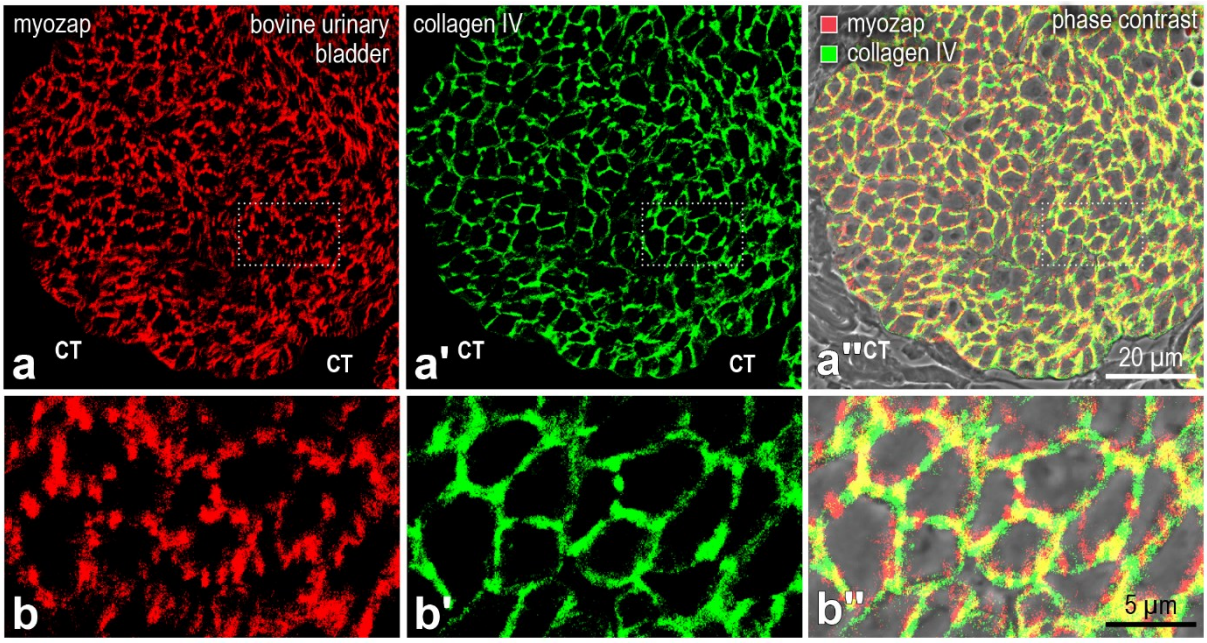


Fig. S2. Myozap and collagen IV show different distribution patterns at cell-cell borders of smooth muscle cell bundles in bovine urinary bladder. (see corresponding Fig. 1f-f'')

Double-label immunofluorescence micrographs show the colocalization of protein myozap (monoclonal murine antibodies; **a**; red) and the basement membrane-specific protein collagen IV (rabbit polyclonal antibodies; **a'**; green) in a cross section of a smooth muscle cell bundle. The overlay of both is presented together with the phase contrast image in (**a''**). The boxed areas are depicted in (**b**-**b''**) at higher magnification below. Note the dotted distribution of myozap in contrast to the continuous distribution of collagen IV at cell-cell borders. Note also the frequent "merger-like" interaction, resulting from the very close association of myozap and the extracellular basal lamina protein collagen IV. CT, connective tissue.

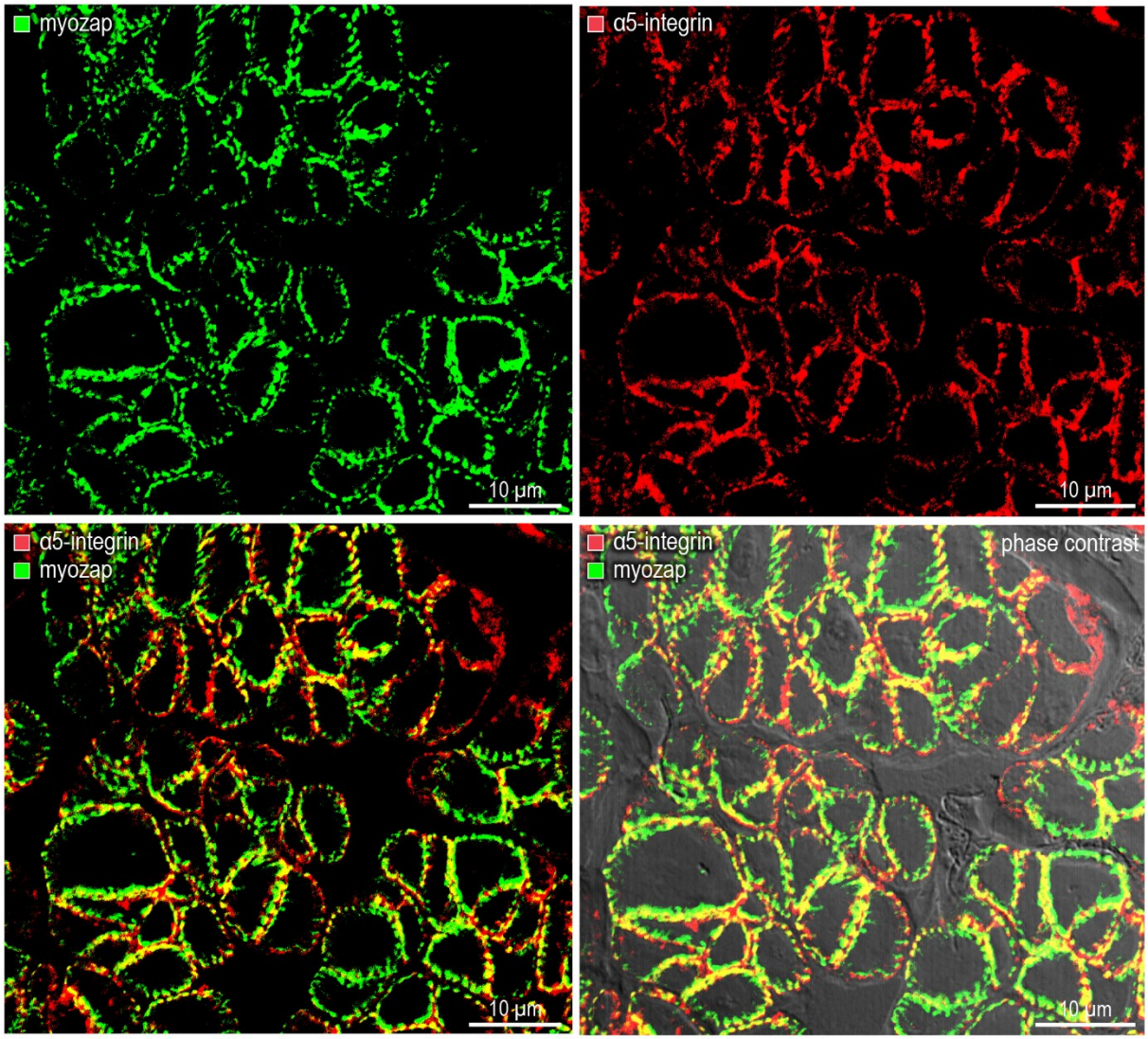


Fig. S3. Myozap co-localizes with α5-integrin in human bladder muscular wall. (see corresponding Fig. 7a)

Note that the cytoplasmic plaque protein myozap (top left; guinea pig antibodies; green) is closely associated with the major focal adhesion transmembrane glycoprotein α5-integrin/CD49e (top right; murine monoclonal antibodies; red). Lower left, merged fluorescence images; lower right, merged fluorescence images and phase contrast recording.

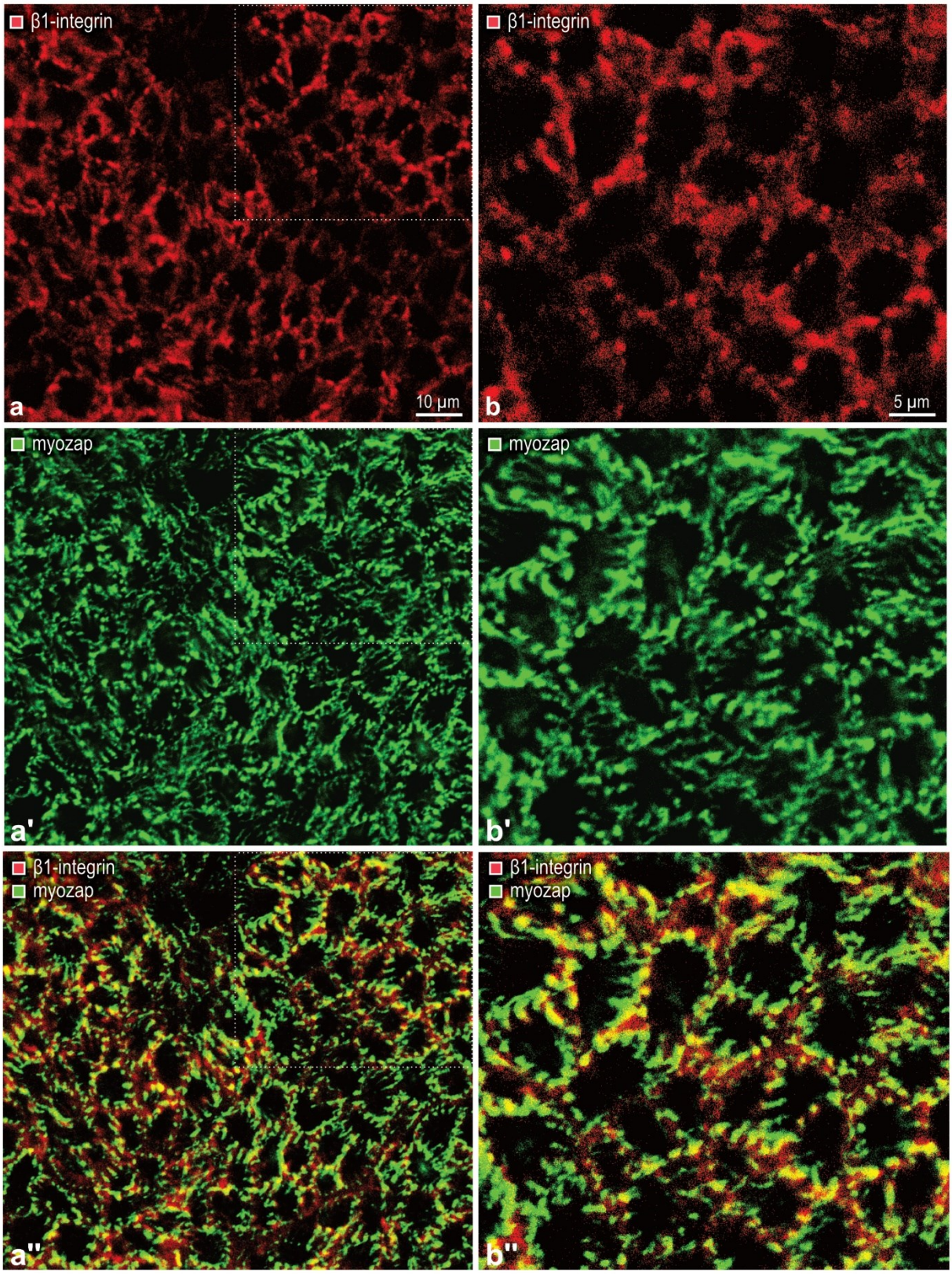


Fig. S4. Myozap co-localizes with β1-integrin in human bladder muscular wall. (see corresponding Fig. 7b)

Note that the major focal adhesion transmembrane glycoprotein β1-integrin (**a**; murine monoclonal antibodies; red) is closely associated in most areas with the cytoplasmic plaque protein myozap (**a'**; guinea pig antibodies; green). Merged image in **(a'')**. Higher magnification of the boxed areas are shown in **(b-b'')**.

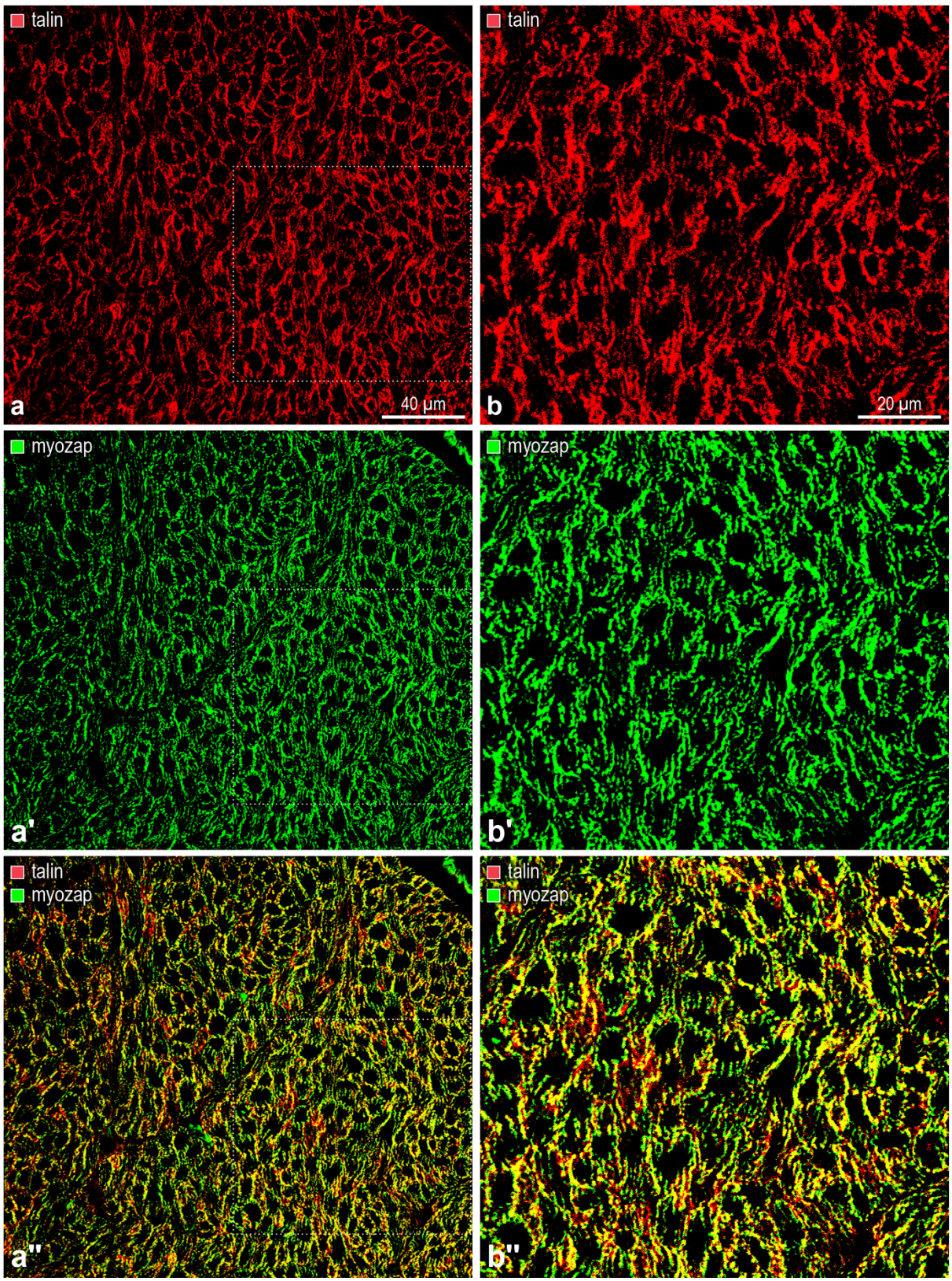


Fig. S5. Myozap co-localizes with talin in bovine bladder muscular wall. (see corresponding Fig. 7d)

A close correlation is observed for the focal adhesion plaque protein talin (**a**; mouse monoclonal antibodies; red) and myozap (**a'**; guinea pig antibodies; green). **(a'')** merged image. **(b-b'')** depict high magnifications of the boxed areas.

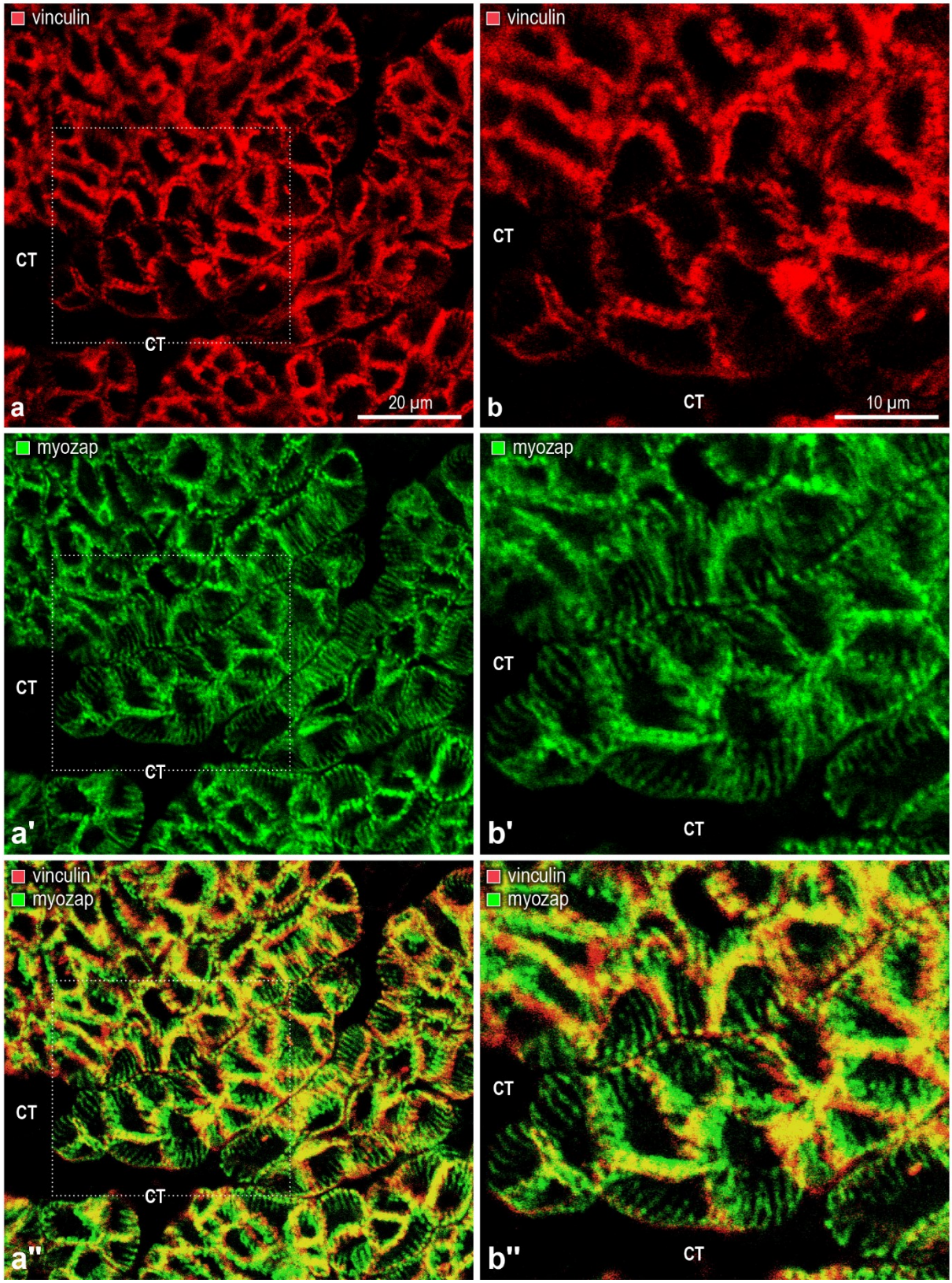


Fig. S6. Myozap partially co-localizes with vinculin in human bladder muscular wall. (see corresponding Fig. 7e)

A partial correlation is observed for the focal adhesion plaque protein vinculin (**a**; mouse monoclonal antibodies; red) and myozap (**a'**; guinea pig antibodies; green). **(a'')** merged image. **(b-b'')** depict high magnifications of the boxed areas. CT, connective tissue.

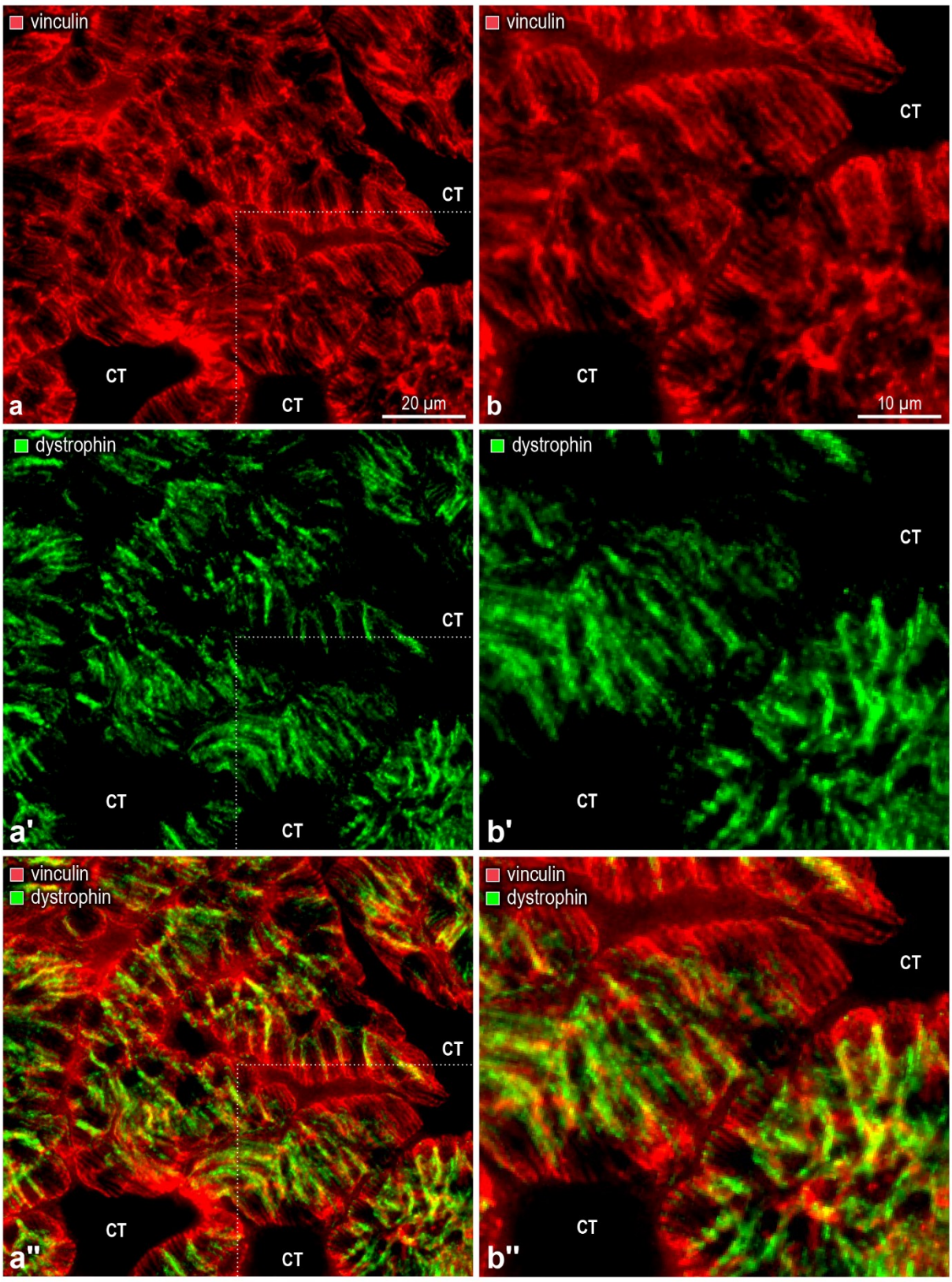


Fig. S7. Dystrophin does not co-localize with vinculin in human bladder muscular wall. (see corresponding Fig. 7f)

Double-label immunofluorescence microscopy of a cryostat section shows the distribution of vinculin (**a**; mouse monoclonal antibodies; red) and dystrophin (**a'**; rabbit polyclonal antibodies; green). **(a'')** merged image. **(b-b'')** depict high magnifications of the boxed areas. Note the different distribution patterns of dystrophin and vinculin.